Virology 452-453 (2014) 264–278

Contents lists available at ScienceDirect

Virology

journal homepage: www.elsevier.com/locate/yviro

The coat protein of *Alternanthera mosaic virus* is the elicitor of a temperature-sensitive systemic necrosis in *Nicotiana benthamiana*, and interacts with a host boron transporter protein

Hyoun-Sub Lim [a], Jiryun Nam [a,1], Eun-Young Seo [a], Moon Nam [a], Anna Maria Vaira [b,c], Hanhong Bae [d], Chan-Yong Jang [a,2], Cheol Ho Lee [e], Hong Gi Kim [a], Mark Roh [b,f,3], John Hammond [b,*]

[a] Department of Applied Biology, Chungnam National University, Daejeon 305-764, Republic of Korea
[b] Floral and Nursery Plants Research Unit, US National Arboretum, USDA-ARS, 10300 Baltimore Avenue B-010A, Beltsville, MD 20705, USA
[c] Istituto di Virologia Vegetale, CNR, Strada delle Cacce 73, Torino 10135, Italy
[d] School of Biotechnology, Yeungnam University, Geongsan 712-749, Republic of Korea
[e] Department of Chemical and Biological Engineering, Seokyoung University, Seoul 136-704, Republic of Korea
[f] Laboratory of Floriculture and Plant Physiology, School of Bio-Resource Science, Dankook University, Cheonan, Chungnam 330-714, Republic of Korea

ARTICLE INFO

Article history:
Received 9 August 2013
Returned to author for revisions
1 September 2013
Accepted 25 January 2014
Available online 17 February 2014

Keywords:
Potexvirus
Host–pathogen interaction
Alternanthera mosaic virus
Systemic necrosis
Protein–protein interactions
Coat protein
Boron transporter

ABSTRACT

Different isolates of *Alternanthera mosaic virus* (AltMV; *Potexvirus*), including four infectious clones derived from AltMV-SP, induce distinct systemic symptoms in *Nicotiana benthamiana*. Virus accumulation was enhanced at 15 °C compared to 25 °C; severe clone AltMV 3-7 induced systemic necrosis (SN) and plant death at 15 °C. No interaction with potexvirus resistance gene *Rx* was detected, although SN was ablated by silencing of *SGT1*, as for other cases of potexvirus-induced necrosis. Substitution of AltMV 3-7 coat protein (CP_{SP}) with that from AltMV-Po (CP_{Po}) eliminated SN at 15 °C, and ameliorated symptoms in *Alternanthera dentata* and soybean. Substitution of only two residues from CP_{Po} [either MN(13,14)ID or LA(76,77)IS] efficiently ablated SN in *N. benthamiana*. CP_{SP} but not CP_{Po} interacted with Arabidopsis boron transporter protein AtBOR1 by yeast two-hybrid assay; *N. benthamiana* homolog NbBOR1 interacted more strongly with CP_{SP} than CP_{Po} in bimolecular fluorescence complementation, and may affect recognition of CP as an elicitor of SN.

Published by Elsevier Inc.

Introduction

Variations in host range and symptom expression between isolates of a single virus species, including potexviruses, are common; a single amino acid (aa) in the RNA-dependent RNA polymerase (RdRp) affects systemic necrosis (SN) in *Nicotiana benthamiana* for both *Potato virus X* (PVX; Kagiwada et al., 2005) and *Plantago asiatica mosaic virus* (PlAMV; Ozeki et al., 2006). The symptom differences between PVX isolates differing by one aa in the C-terminal domain of RdRp were not related to virus accumulation (Kagiwada et al., 2005). However, it has recently been shown that the single aa difference in the polymerase (POL) domain of PlAMV has a significant effect on virus replication, but that it is actually the helicase (HEL) domain of the PlAMV RdRp that is the elicitor of the SN response, and that the HEL domain of an asymptomatic isolate of PlAMV can induce SN following high-level expression by agroinfiltration (Komatsu et al., 2011).

The potato gene *Rx* normally confers extreme resistance to PVX, mediated by recognition of coat protein (CP) residues 121 and 127 (Goulden et al., 1993); isolates with 121(K)/127(R) overcome the resistance (Bendahmane et al., 1995). *Rx* limits accumulation of PVX in the inoculated cells and protoplasts without induction of a local hypersensitive response (HR) in potato, *Nicotiana tabacum* or *N. benthamiana*, yet can induce a separate cell death response following agroinfiltration of the elicitor CP (Bendahmane et al., 1999). A systemic HR (sHR) may occur when there is a low-affinity

* Corresponding author. Tel.: +1 301 504 5313; fax: +1 301 504 5096.
E-mail addresses: hyounlim@cnu.ac.kr (H.-S. Lim), jilyoon@naver.com (J. Nam), sey22@cnu.ac.kr (E.-Y. Seo), moonlit51@cnu.ac.kr (M. Nam), a.vaira@ivv.cnr.it (A.M. Vaira), hanhongbae@ynu.ac.kr (H. Bae), sunbispirit@gmail.com (C.-Y. Jang), chlee1219@hanmail.net (C.H. Lee), hgkim@cnu.ac.kr (H.G. Kim), marksroh@gmail.com (M. Roh), john.hammond@ars.usda.gov (J. Hammond).
[1] Current address: Department of Bioscience II, Bio-Medical Science, Daejeon 305-301, Republic of Korea.
[2] Current address: Department of Plant Pathology, University of Kentucky, Lexington, KY 40546, USA.
[3] Retired.

http://dx.doi.org/10.1016/j.virol.2014.01.021
0042-6822 Published by Elsevier Inc.

interaction between elicitor and receptor, or when the elicitor is produced late in the infection cycle (Bendahmane et al., 1999), in cases where infection is usually locally limited (e.g. Dinesh-Kumar et al., 2000, Seo et al., 2009). Rx is a coiled-coil/nucleotide binding site/leucine rich repeat (CC–NBS–LRR) protein, and interactions between CC and LRR domains mediated by PVX CP are necessary to induce resistance-related cell death (Moffett et al., 2002). An sHR response was observed in *Rx*-transgenic *N. benthamiana* only when RanGap2 expression was silenced, presumably due to decreased efficiency of recognition of the PVX CP elicitor, or of downstream signaling, resulting in activation of the resistance mechanism too slowly to prevent spread of the pathogen (Tameling and Baulcombe, 2007) and allowing necrosis to occur as a secondary resistance response (Bendahmane et al., 1995). Rx-mediated extreme resistance to PVX in *N. benthamiana* is dependent on expression of ubiquitin ligase-associated protein SGT1 (Peart et al., 2002), and on a number of other genes including *Hsp90*, *Rar1*, *RanGap1*, *RanGap2*, and *Ago4* (Azevedo et al., 2002, 2006; Bhattacharjee et al., 2009; Sturbois et al., 2012; Tameling and Baulcombe, 2007; Tameling et al., 2010).

Although *Rx* was initially identified as conferring race-specific resistance against PVX, more recent work has shown that it can confer either extreme or variable resistance to several other potexviruses lacking significant CP amino acid homology to PVX, suggesting that a conserved structural element rather than a specific sequence controls the *Rx* response (Baurès et al., 2008; Candresse et al., 2010). Interactions with additional host factors may also be required for the induction of *Rx*-mediated resistance (Baurès et al., 2008; Sturbois et al., 2012), and it is likely that this is also true of other resistance genes.

Different virus–host interactions may lead to necrosis. Many viruses induce necrotic local lesions, which often prevent systemic movement; examples are local limitation of TMV in *N. tabacum* carrying the *N* gene (Padgett et al., 1997), or *Nicotiana sylvestris* bearing the *N′* gene (Taraporewala and Culver, 1996). In other cases systemic infection is typically accompanied by necrosis, as with *Tomato bushy stunt virus* infection of *Nicotiana* species including *N. benthamiana* (Scholthof et al., 1995). Only certain isolates of a virus may induce SN in a particular host, and both timing and severity of necrosis may be affected by environmental conditions; induction of SN in *Nicotiana clevelandii* by *Cauliflower mosaic virus* (CaMV) isolate W260, for example, is more intense under low light, low temperature, and short-day conditions (Király et al., 1999). An sHR may also occur in some virus:host combinations under appropriate environmental conditions; for example, the *N. tabacum N* gene-mediated response to TMV is temperature sensitive, and TMV spreads systemically in plants maintained at 30 °C, and sHR occurs on shifting plants to 20 °C, but only in areas where active replication is occurring (Someya et al., 2004).

Alternanthera mosaic virus (AltMV) is a potexvirus closely related to *Papaya mosaic virus* (PapMV), and was originally reported from the weed *Alternanthera pungens* (Geering and Thomas, 1999). AltMV naturally infects various ornamentals, including several *Phlox* species (Hammond et al., 2006a, 2006b), *Portulaca* (Ciuffo and Turina, 2004; Hammond et al., 2006a, 2006b; Baker et al., 2006), *Scutellaria* and *Crossandra* (Baker et al., 2006), and *Angelonia* (Lockhart and Daughtrey, 2008). *Arabidopsis thaliana* is an experimental host in which no obvious symptoms are apparent (Lim et al., 2010b). In *N. benthamiana*, phlox isolates AltMV-SP and AltMV-PA produce chlorotic local lesions and systemic mosaic, whereas portulaca isolate AltMV-Po produces milder symptoms (Hammond et al., 2006b). At low temperatures (15–20 °C) AltMV-SP and AltMV-PA produce necrotic local lesions and severe SN (Hammond et al., 2006a). Three geographically distinct isolates from portulaca share several CP aa residues that distinguish them from phlox and alternanthera isolates (Hammond et al., 2006a; and FJ822136). We have created biologically distinct infectious clones from AltMV-SP; both the RdRp POL domain and TGB1 of these clones contribute to symptom severity, and significantly affect AltMV accumulation (Lim et al., 2010a). We report here interactions between AltMV and *N. benthamiana,* in which SN occurs primarily at low temperatures and high levels of viral replication of variants having a CP competent to induce necrosis. SN was correlated with particular CP aa residues, and was ablated when *SGT1* was silenced, but was not found to be affected in *Rx*-transgenic *N. benthamiana*. Only the CP competent to induce necrosis was found to interact strongly with a host boron transporter protein, which may act as a host factor involved in recognition of the CP elicitor of SN.

The boron transporter of *A. thaliana* (AtBOR1) is reported to localize to the plasma membrane, to regulate boron loading of the xylem especially in the roots, and to protect shoots from boron toxicity (Takano et al., 2002). Boron is an essential element for plant growth, but either excess or deficiency outside a narrow physiological concentration range can cause damage including tissue necrosis (Cakmak and Römheld, 1997; Nable et al., 1997; Takano et al., 2005). When boron is available in excess, AtBOR1 is normally tightly regulated by transport to the vacuole for degradation (Takano et al., 2005). It is possible that interaction with CP interferes with BOR1 regulation and/or boron transport to induce necrosis, or that the interaction modulates response of an *R* gene.

Results

AltMV CP is a determinant of systemic necrosis in N. benthamiana

We have previously demonstrated that infectious clones of four sequence variants derived from AltMV-SP differ in symptom severity on *N. benthamiana*, and that symptom expression of AltMV-SP and each of the infectious clones is enhanced at 15 °C compared to 25 °C; all four sequence variants share an identical CP sequence (Lim et al., 2010a). The infectious clone with the highest level of replication, AltMV 3-7, frequently causes necrosis at 25 °C and at 15 °C reliably causes systemic necrosis by 10 dpi, typically killing plants by 30 dpi (Table 1; Lim et al., 2010a). In contrast, we have previously shown that AltMV-Po produces mild mosaic (Hammond et al., 2006b), while at 15 °C symptoms are more severe but without inducing necrosis (Table 1). The 3′-terminal region of AltMV-Po (AY850930) differs from AltMV 3-7 (identical in this region to AltMV 4-7; GQ179647) by one aa at the C-terminus of TGB1, six aa in TGB2, four aa in TGB3 and nine aa in CP. To determine whether TGB2 and TGB3 affect the observed SN caused by AltMV-SP, AltMV-Po TGB2/3 was substituted into 3-7 (Fig. 1A). The exchange mutant 3-7$_{Po\text{-}TGB23}$ induced symptoms in *N. benthamiana* equivalent to 3-7 (Table 1).

Next, we substituted AltMV-Po CP into 3-7:MCS to form 3-7$_{Po\text{-}CP}$ (Fig. 1A). The nine aa differences between AltMV-Po and AltMV-SP are mainly in the N-terminal half of the CP, with residues 13 and 14 predicted to be exposed on the virion surface by comparison with the PVX CP structure of Dobrov et al. (2007). In *N. benthamiana*, 3-7$_{Po\text{-}CP}$ induced only mild mosaic, without necrosis even 30 dpi at 15 °C (Fig. 1B; Table 1). As the symptoms in *N. benthamiana* were similar to those induced by AltMV-Po, effects in other hosts were also examined in comparison to AltMV 3-7. In *Alternanthera dentata*, 3-7 caused local lesions, stunting, and early anthocyanin production, whereas 3-7$_{Po\text{-}CP}$ was symptomless (Fig. 1B). In soybean, 3-7 induced severe necrosis on the trifoliate leaf developing first after inoculation, whereas 3-7$_{Po\text{-}CP}$ caused no obvious symptoms in the first trifoliate leaf despite producing equivalent CP levels (Fig. 1B); western blotting showed that 3-7$_{Po\text{-}CP}$, but not 3-7, caused further symptomless systemic infection

Table 1
Symptoms induced by AltMV variants in *Nicotiana benthamiana* at 25 °C and 15 °C.

Virus variant	CP isoelectric point	Systemic symptoms	
		25 °C	15 °C
3-7		Mosaic, localized necrosis[a]	Systemic necrosis, dead < 30 dpi[b]
3-7-MCS	5.73	Mosaic, localized necrosis	Systemic necrosis, dead < 30 dpi
AltMV-Po	5.716	Mild mosaic	Mosaic
$3\text{-}7_{PoTGB2/3}$	5.73	Mosaic, localized necrosis	Systemic necrosis, dead < 30 dpi
$3\text{-}7_{Po\text{-}CP}$	5.716	Mild mosaic	Mosaic
$3\text{-}7_{MN(13,14)ID}$	5.212	Mild mosaic	Mosaic
$3\text{-}7_{N(36)S}$	5.73	Mosaic, localized necrosis	Systemic necrosis, dead < 30 dpi
$3\text{-}7_{T(66)A}$	5.73	Mosaic, localized necrosis	Systemic necrosis, dead < 30 dpi
$3\text{-}7_{A(69)V}$	5.73	Mosaic, localized necrosis	Systemic necrosis, dead < 30 dpi
$3\text{-}7_{LA(76,77)IS}$	5.73	Mild mosaic	Mosaic
$3\text{-}7_{E(78)G}$	7.026	Mosaic, localized necrosis	Systemic necrosis, dead < 30 dpi
$3\text{-}7_{T(154)A}$	5.73	Mosaic, localized necrosis	Systemic necrosis, dead < 30 dpi
$3\text{-}7_{MN(13,14)ID+LA(76,77)IS}$	5.212	Mild mosaic	Mild mosaic

[a] Areas of necrosis were observed within the leaf lamina, in the petiole, and sometimes in the stem.
[b] Necrosis affecting the apex and entire leaves and petioles.

(data not shown). RNA levels were analyzed from leaves of individual *N. benthamiana* by quantitative real-time RTPCR (Q-RTPCR) at 10 dpi (before induction of systemic necrosis by 3-7); no statistically significant difference was observed between 3-7 and $3\text{-}7_{Po\text{-}CP}$ accumulation at either 15 °C or 25 °C, although each accumulated to approximately 4 × higher levels at 15 °C than at 25 °C (Fig. 1C).

It is known that CP mutations can influence both subunit–subunit interactions and symptom expression of TMV (Culver et al., 1994; Taraporewala and Culver, 1996). When 3-7 and $3\text{-}7_{Po\text{-}CP}$ were extracted from *N. benthamiana* leaves in the presence or absence of β-mercaptoethanol, western blotting after separation on non-denaturing gels revealed a CP dimer band as well as monomer for 3-7, but only monomer for $3\text{-}7_{Po\text{-}CP}$ (Fig. 1D).

PVX overexpression of AltMV-SP CP, but not AltMV-Po CP, induces systemic necrosis

We confirmed the activity of AltMV-SP as an elicitor of systemic necrosis by expression from a PVX vector as an added gene (Fig. 2A). Plants of *N. benthamiana* were separately inoculated with transcripts of pPVX-MCS, pPVX-CP_{SP}, or pPVX-CP_{Po}, and grown at either 15 °C or 25 °C. We also expressed CP_{SP} and CP_{Po} by agroinfiltration with pGD:CP_{SP} or pGD:CP_{Po}, and separately infiltrated pGD (Goodin et al., 2002) as a control; all constructs were infiltrated in the presence of pGD:p19 to minimize silencing of the constructs. No necrosis was observed in any CP-agroinfiltrated leaves, even when plants were grown at 15 °C after agroinfiltration. Agroinfiltrated tissues developed chlorosis by 7 days after infiltration (sooner at 25 °C than at 15 °C), and began to collapse within about 2 weeks after infiltration without any obvious distinction of response between pGD:CP_{SP} or pGD:CP_{Po}; control leaves infiltrated with pGD (the empty vector) developed chlorosis and collapsed in a similar manner (Supplemental Fig. 1, and data not shown). Although AltMV accumulates to approximately 4–5-fold higher levels at 15 °C than at 25 °C (Fig. 1C; Lim et al., 2010a), no such increase in expression was detected at 15 °C following agroinfiltration of pGD:CP_{SP} or pGD:CP_{Po} (Supplemental Fig. 1). Western blotting indicated that AltMV CP expression from PVX was at a much higher level than in agroinfiltrated tissue (Fig. 2B), and Q-RTPCR showed the AltMV CP RNA level expressed from PVX or in AltMV-infected leaves to be ca. 200-fold higher than in agroinfiltrated tissue (data not shown). Plants infected with PVX-MCS developed systemic mosaic in upper leaves, with somewhat increased severity at 15 °C, while PVX-CP_{Po} produced similar symptoms (Fig. 2C and D). In contrast, plants infected with PVX-CP_{SP} developed interveinal necrosis in upper leaves at 25 °C, and veinal-associated systemic necrosis at 15 °C starting at about 2 weeks after infection (Fig. 2C and D).

Homologous interaction strength of CP_{SP} and CP_{Po} differs significantly

To further examine CP subunit interactions, we expressed CP_{SP} and CP_{Po} separately as fusions to the Gal4 AD and BD (James et al., 1996). Yeast cotransformed with AD:CP_{SP} and BD:CP_{SP} exhibited strong growth within 40 h, indicating strong interactions between these proteins; there were no false positives when AD or BD was paired with AD:CP or BD:CP for either CP_{SP} or CP_{Po} (Table 2). When yeast were cotransformed with AD:CP_{Po} and BD:CP_{Po}, very weak growth was observed at 80 h, indicating weak homologous interaction (Table 2).

Differential binding in yeast two-hybrid experiments may not quantitatively reflect interactions *in vivo*; however, we have previously demonstrated that interactions between different ratios of agroinfiltrated *Barley stripe mosaic virus* (BSMV) TGB2 and TGB3 affect subcellular localization in a manner that reflects the expression ratios of wt BSMV infections (Lim et al., 2009). CP_{SP} and CP_{Po} were therefore separately subcloned into pGD (unfused CP) and pGDG (GFP:CP fusions) for agroinfiltration (Fig. 3A). Equal concentrations (0.4 OD_{600}) of *Agrobacterium* containing pGDG:CP_{SP} and pGDG:CP_{Po} were infiltrated. Equivalent total levels of agrobacteria were infiltrated by inclusion of cultures of pGD vector control as necessary; [pGDG:CP_{SP} and pGD:CP_{SP} plus pGD] was infiltrated into the left half of leaves, and in order to increase the total CP concentration [pGDG:CP_{SP} and 2 × pGD:CP_{SP}] was infiltrated into the right half (Fig. 3A). Mixtures of pGDG:CP_{Po} and pGD:CP_{Po} were similarly infiltrated. Western blots showed that GFP:CP fusions migrated at the anticipated size; both western blots and Q-RTPCR showed CP expression proportional to the amount of pGD:CP added (Fig. 3B and C; and data not shown). Each GFP–CP fusion localized to the cell wall at low total CP concentration; however at increased total CP concentration (pGDG:CP_{SP}+2 × pGD:CP_{SP}), CP_{SP} aggregated primarily in fewer, larger, punctate foci rather than at the cell wall (Fig. 3B, top). Even at increased total CP levels, pGDG:CP_{Po} remained localized at the cell wall and small foci dispersed in the cytoplasm (Fig. 3B, bottom). No necrosis was observed in any CP-agroinfiltrated leaves.

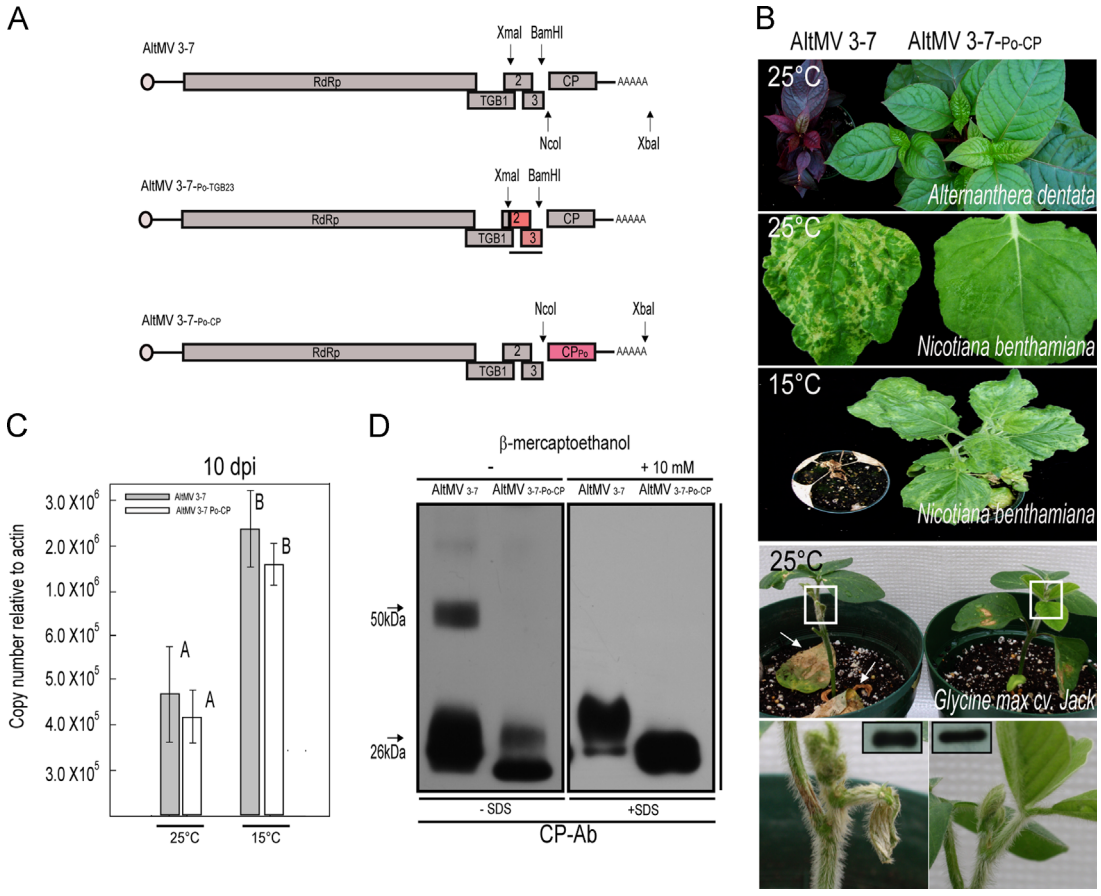

Fig. 1. Effects of substitution of the AltMV-Po TGB2/3 and CP into AltMV 3-7. (A) Substitution of the AltMV-Po TGB2/3 and CP into AltMV 3-7. Schematic diagram of AltMV 3-7 (top), and substitutions of the AltMV-Po TGB2/3 to form AltMV 3-7$_{Po\text{-}TGB2/3}$ (middle) and AltMV Po-CP to form AltMV 3-7$_{Po\text{-}CP}$ (bottom). (B) RNA transcripts were inoculated to *N. benthamiana*, *Alternanthera dentata,* and *Glycine max* (soybean). By 30 dpi 3-7 induced severe symptoms in *N. benthamiana* and *A. dentata*, and necrosis of the second trifoliate soybean leaf by 10 dpi. 3-7$_{Po\text{-}CP}$ produced mild symptoms at 25 °C, without necrosis at 15 °C in *N. benthamiana*, and mild symptoms in *A. dentata* and *G. max*. The soybean trifoliate leaf indicated by the white square is shown magnified below; (insets) CP-Ab reactions with extracts of the soybean leaves pictured. (C) Q-RTPCR of 3-7 and 3-7$_{Po\text{-}CP}$ at 10 dpi in *N. benthamiana* at 15 °C and 25 °C, normalized to actin. Results with the same letter are not statistically different (P=0.05). (D) Western blot of protein extracts from AltMV 3-7 and AltMV3-7$_{Po\text{-}CP}$ with (left) or without (right) 10 mM β-mercaptoethanol separated on a 12% non-denaturing gel, probed with anti-AltMV antibody. Note that the predicted molecular weight of 3-7 CP is 22,231, whereas that of CP$_{Po}$ is 22,099, with pI of 5.73 and 5.716 respectively (Table 2).

We used modified *Agrobacterium*-mediated transient expression plasmids (Deng et al., 2007) to develop a GST affinity chromatography system using proteins expressed *in planta*. Unfused CP$_{SP}$ was coexpressed with GST or GST:CP$_{SP}$, and CP$_{Po}$ with GST:CP$_{Po}$ (Fig. 4A and, B lanes 1–3) in *N. benthamiana*, and GST pull-down experiments were performed. Native CP$_{SP}$ did not bind to the matrix when coexpressed with GST, nor CP$_{Po}$ with GST:CP$_{Po}$ (Fig. 4B, lanes 1 and 3 bottom), but CP$_{SP}$ was retained when coexpressed with GST:CP$_{SP}$ (Fig. 4B, lane 2 bottom). A western blot of GST:CP fusions separated in a non-denaturing gel showed a dimer of GST:CP$_{SP}$, but not of GST:CP$_{Po}$ (Fig. 4C). These results demonstrated formation of strong homologous CP$_{SP}$:CP$_{SP}$ (but not CP$_{Po}$:CP$_{Po}$) binding and confirmed the yeast two-hybrid CP-CP interactions.

The PVX resistance gene Rx does not confer resistance to AltMV, but necrosis is ablated by silencing of NbSGT1

The resistance gene *Rx* was originally thought to be specific (and race-specific) for PVX (e.g. Goulden et al., 1993), but has more recently been shown to confer either extreme or variable resistance against other potexviruses lacking significant CP aa homology to PVX (Baurès et al., 2008; Candresse et al., 2010). We therefore challenged *Rx*-transgenic *N. benthamiana* with AltMV to determine whether *Rx* prevented systemic infection and/or SN. When 3-7 or 3-7$_{Po\text{-}CP}$ were inoculated to PVX-resistant *Rx*-transgenic *N. benthamiana* line Rx-18, systemic mosaic symptoms typical of infections of wild-type plants were observed at both 25 °C and 15 °C, followed by SN at 15 °C in plants inoculated with AltMV 3-7 (Supplemental Fig. 2); in contrast PVX infected wild-type but not Rx-18 *N. benthamiana*, inducing severe mosaic without necrosis at 15 °C (Supplemental Fig. 2).

SGT1 is involved in disease resistance in barley, where *SGT1* silencing compromised powdery mildew resistance mediated by CC–NBS–LRR protein Mla6 (Azevedo et al., 2002). NbSGT1 is required for *Rx* mediated resistance, and *NbSGT1* silencing compromised cell death (HR) associated with diverse other resistance (*R*) genes (Peart et al., 2002). To investigate whether AltMV-induced necrosis involves interaction with an *R* gene, non-transgenic *N. benthamiana* were first infected with a TRV vector carrying a fragment of *NbSGT1.1* (TRV:SGT); then 3-7 inoculated 20 dpi after TRV:SGT agroinfiltration, at 25 °C. In control plants infected with TRV:Sulfur (Fitzmaurice et al., 1999), gene silencing was obvious by 20 dpi (Supplementary Fig. 3A); additional controls were inoculated with TRV vector lacking insert (TRV:00). Growth of plants inoculated with empty vector TRV:00 was similar to that of plants infected with TRV:Sulfur (Supplementary Fig. 3A and B), indicating that unlike the effects reported in vacuum-infiltrated young seedlings (Hartl et al., 2008), the empty vector did not negatively affect plant growth compared to the silencing

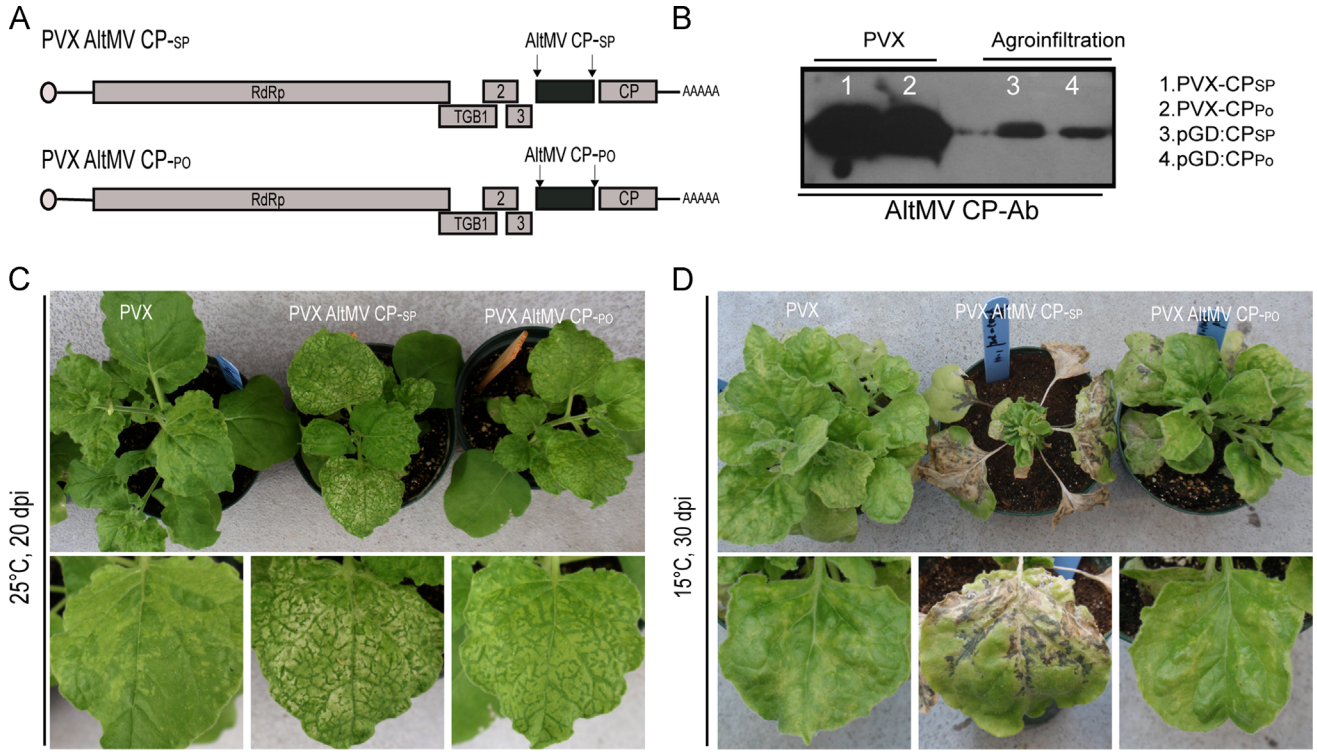

Fig. 2. Symptoms induced by PVX overexpressing AltMV CP_{SP} or CP_{Po}. (A) PCR amplified AltMV CP was inserted into the MCS of a modified PVX infectious clone (Lim et al., 2010b). (B) Protein expression was compared between PVX and agroinfiltration. Tissues were collected from $PVX_{CP\text{-}SP}$ and $PVX_{CP\text{-}Po}$ infected non-transgenic *N. benthamiana* plants at 20 dpi, and pGD-CP_{SP} and pGD-CP_{Po} agroinfiltrated tissue collected at 3 dpi; both sets of plants were maintained at 25 °C. A western blot of proteins from 100 mg of leaves, separated on a 12% SDS-polyacrylamide gel, was developed with AltMV-specific antibody. Lanes (1) PVX-CP_{SP}, (2) PVX-CP_{Po}, (3) pGD-CP_{SP}, and (4) pGD-CP_{Po}. (C and D) Symptoms of *N. benthamiana* inoculated with transcripts of PVX (left), PVX-CP_{SP} (center), and PVX-CP_{Po} (right) at (C) 25 °C, shown at 20 dpi and (D) 15 °C, shown at 30 dpi.

Table 2
Yeast two hybrid analysis of AltMV CP interactions.

BD fusion	AD fusion	Interaction
CP_{SP}	AD	–[a]
BD	CP_{SP}	–
CP_{SP}	CP_{SP}	++++[b]
CP_{Po}	AD	–
BD	CP_{Po}	–
CP_{Po}	CP_{Po}	+[c]
$CP_{MN(13,14)ID}$	$CP_{MN(13,14)ID}$	++++
$CP_{N(36)S}$	$CP_{N(36)S}$	++++
$CP_{T(66)A}$	$CP_{T(66)A}$	++++
$CP_{A(69)V}$	$CP_{N(36)S}$	++++
$CP_{LA(76,77)IS}$	$CP_{LA(76,77)IS}$	+
$CP_{E(78)G}$	$CP_{E(78)G}$	++++
$CP_{T(154)A}$	$CP_{T(154)A}$	++++

[a] Yeast growth not detected.
[b] Yeast growth detected after 20 h incubation.
[c] Yeast growth detected after 80 h incubation.

constructs. *N. benthamiana* infected with TRV:SGT were shorter and more branched than TRV:00-infected controls (Peart et al., 2002), but neither showed necrosis in the absence of AltMV infection (Supplementary Fig. 3B and C). Silencing of *NbSGT1* ablated necrosis induced by 3-7 infection at both 25 °C and 15 °C, while severe necrosis developed in TRV:00 controls infected with 3-7 (Fig. 5A and B; Supplementary Fig. 3D and E). AltMV levels were not statistically different between TRV:SGT and TRV:00 inoculated plants (Supplementary Fig. 3F). These results suggest that AltMV-induced necrosis is caused by recognition of CP_{SP} by an *R* gene distinct from *Rx*. Q-RTPCR indicated that 3-7 accumulation at 25 °C was similar between *NbSGT1*-silenced and TRV:00-infected plants (Fig. 5C), while *NbSGT1* transcript levels in silenced *N. benthamiana* were only 10–15% of those of controls (Fig. 5D); however, AltMV necrosis was eliminated by *NbSGT1* silencing. It was not possible to compare 3-7 accumulation levels at 15 °C, as the upper leaves of TRV:00 plants were necrotic prior to the 20 dpi sampling point, precluding extraction of RNA.

Substitution of AltMV-Po CP residues identifies AltMV-SP residues involved in CP-mediated induction of necrosis

Eight mutants substituting different AltMV-Po residues into the CP_{SP} were used to examine the influence of these residues on induction of necrosis (Fig. 6A). Transcripts of infectious clones bearing CP mutants MN(13,14)ID, N(36)S, T(66)A, A(69)V, LA (76,77)IS, E(78)G, T(154)A, and MN(13,14)ID+LA(76,77)IS were inoculated to *N. benthamiana* and plants incubated at either 15 °C or 25 °C; all of the mutants infected *N. benthamiana* systemically. Mutants N(36)S, T(66)A, A(69)V, E(78)G and T(154)A induced necrosis, with systemic necrosis and death at 15 °C, as for the parental isolate AltMV 3-7; in contrast, no necrosis occurred with MN(13,14)ID, LA(76,77)IS, or MN(13,14)ID+LA(76,77)IS (Fig. 6A, Table 1), as with AltMV 3-$7_{Po\text{-}CP}$ (Fig. 1B). Q-RTPCR showed that accumulation levels of the non-necrotic mutants were equivalent (Fig. 6B). Electrophoretic migration of all of the mutant CPs was similar to that of CP_{SP} (Fig. 6B), although CP_{Po} (predicted MW 22,099) migrated slightly faster than CP_{SP} (predicted MW 22,231; see Fig. 1D). Electron microscopy of sap extracts of plants infected with AltMV 3-7, AltMV-Po, AltMV 3-$7_{Po\text{-}CP}$, or the various CP mutants revealed no obvious differences in particle morphology, flexibility, or stability (Supplementary Fig. 4).

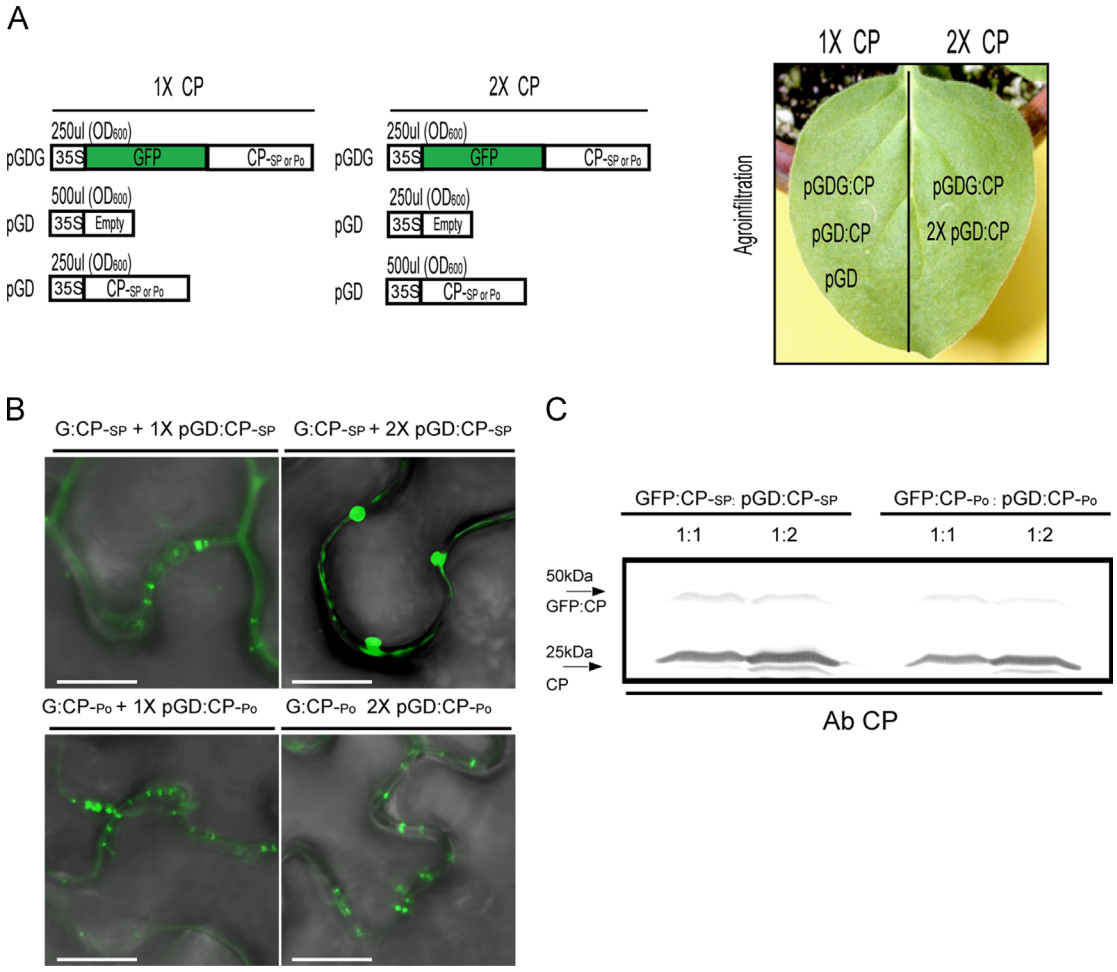

Fig. 3. Subcellular localization and self-interaction of CP_{SP} and CP_{Po}. (A) CP_{SP} and CP_{Po} were separately expressed from pGDG and pGD by agroinfiltration of *N. benthamiana*. Two concentrations of pGD:CP were tested with a constant level of pGDG:CP in opposite half leaves (right). (B) At 36 h GFP was detected in epidermal cells using confocal microscopy. Top: pGDG:CP_{SP}, bottom: pGDG:CP_{Po}. Left: pGDG:CP and pGD:CP at equal concentration, (pGDG:CP[0.4 OD_{600}]+pGD:CP[0.4 OD_{600}]); right: pGDG:CP+2X pGD:CP, (pGDG:CP[0.4 OD_{600}]+pGD:CP[0.4 OD_{600}]+pGD:CP[0.4 OD_{600}]); bar=50 μm. (C) Western blot of proteins from infiltrated leaves, separated on 12% SDS-PAGE, developed with AltMV-specific antibody.

Yeast two-hybrid analysis of these mutants revealed that only $CP_{LA(76,77)IS}$ resulted in weaker CP–CP interactions similar to those observed with CP_{Po} (Table 2).

CP sequence analysis

The predicted CP secondary structure of AltMV-Po differs from that of AltMV-SP, with the greatest differences in the regions around the MN(13,14)ID, LA(76,77)IS, and E(78)G changes. $CP_{MN(13,14)ID}$ was predicted to have N-terminal structure similar to CP_{Po}, while $CP_{LA(76,77)IS}$ and $CP_{E(78)G}$ were predicted to have locally increased proportions of coil or β-strand rather than α-helix compared to CP_{SP}, but not to the extent of CP_{Po}, as only one or two of the three variant residues (ISG) were mutated (data not shown). Differences in predicted hydropathy between CP variants were localized and not pronounced (data not shown). AltMV-Po, MN(13,14)ID, and MN(13,14)ID+LA(76,77)IS had lower CP pI and induced milder symptoms in the absence of necrosis; $CP_{E(78)G}$, the only mutant with higher pI, caused systemic necrosis similar to WT 3-7 (Table 1). However, non-necrotic mutant LA(76,77)IS had a CP pI of 5.73, identical to that of AltMV 3-7, indicating that reduced pI is not necessary for absence of necrosis.

Additional differences between the mutants were noted using ProSite (Bairoch et al., 1997). A CK2 phosphorylation site was predicted at residues 75–78 (SLAE in AltMV-SP and most mutants; SISE in LA(76,77)IS). These residues were SISG in AltMV-Po, and SLAG in E(78)G, in which no phosphorylation site was predicted. A potential myristoylation site (GVSLSQ) was predicted at residues 78–83 only in AltMV-Po and mutant E(78)G, where AltMV-SP and all other mutants have EVSLSQ. None of these differences correlated with necrosis.

By comparison to the structure predicted for PVX CP (Dobrov et al., 2007) AltMV CP lacks domains equivalent to helical domain α2, and β-sheet β1, and α1 is contiguous with α3 (Fig. 6C). AltMV residues MN(13,14) are within surface located β2, and LA(76,77) in the internal loop between α4 and α5 (Fig. 6C).

The crystal structure of residues 6–215 of PapMV CP has recently been determined (Yang et al., 2012), so we were able to use Cn3D to overlay the AltMV CP amino acid sequence onto the PapMV CP structure (Supplemental Figs. 5 and 6) and view the apparent locations of residues that differ between CP_{SP} and CP_{Po}. CP_{SP} residues MN(13,14) are located within α-helix 1, exposed at the virion surface and presumed to bridge neighboring subunits within the same turn of the virion helix (Yang et al., 2012; Supplemental Fig. 7). CP_{SP} residue N36 is in α-helix 2 on the outer surface of the CP subunit, while T66 and A69 are on a subunit surface loop between α-helices 3 and 4, between adjacent turns of the virion helix (Supplemental Fig. 7). Residues LAE(76–78) are to

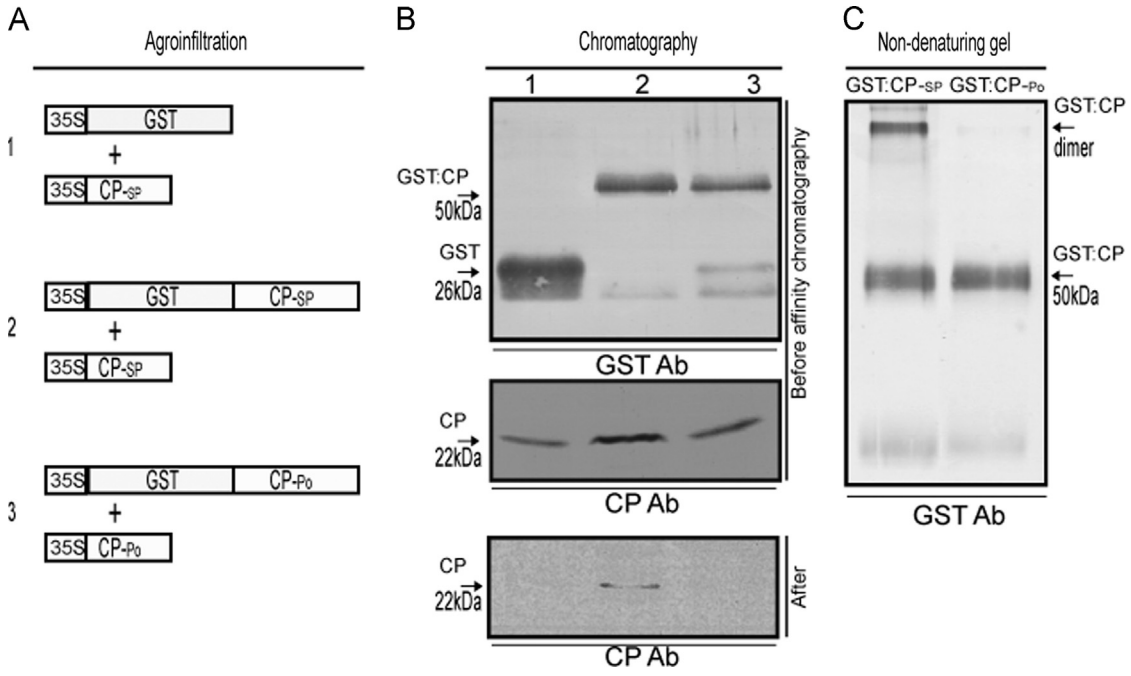

Fig. 4. Glutathione affinity chromatography detection of CP interactions. (A) pGD-CP_{SP} expressed in *N. benthamiana* with (1) pGD-GST or (2) pGD-GST:CP_{SP}; or (3) pGD-CP_{Po} expressed with pGD-GST:CP_{Po}, by agroinfitration. (B) Leaf extracts (see text) were applied to the GSH matrix. Protein eluting from the matrix was separated by 10% SDS-PAGE before (top and middle, crude extracts) and after (bottom, column eluates) glutathione affinity chromatography. Western blots were probed with anti-GST or anti-AltMV antibody. (C) Western blot of GST:CP_{SP} and GST:CP_{Po} extracts separated by 10% non-denaturing gel, probed with anti-GST antibody.

the N-terminal side of α-helix 4, and at the interface between subunits in the same turn of the virion helix (see Figs. 3 and 5 of Yang et al., 2012); finally, residue T154 is on the side of the subunit opposite T66 and A69, again between adjacent turns of the virion helix (Supplemental Fig. 7).

CP_{SP} but not CP_{Po} interacts strongly with a host boron transporter protein

We also utilized the yeast two-hybrid assay to probe an Arabidopsis cDNA library to identify host proteins interacting with CP_{SP}. A positive interaction was found with *A. thaliana* boron transporter 1 (AtBOR1). Subsequent testing with CP_{Po} revealed differential, weaker binding to AtBOR1 (data not shown). The *N. benthamiana* homolog of BOR1 was then amplified using primers based on the *N. tabacum* BOR1 sequence (EU599083), and cloned into pSPYNE173. Bimolecular fluorescence complementation (BiFC) using pSPYNE173:NtBOR1 infiltrated with either pSPYNE(M):CP_{SP} or pSPYNE(M):CP_{Po} demonstrated the interaction of CP with *N. benthamiana* BOR1, but CP_{Po} did not interact with BOR1 (Fig. 7A) when infiltrated at equivalent concentration (Fig. 7B); the BiFC signal was observed at the cell periphery, consistent with the anticipated plasma membrane localization expected for BOR1 (Takano et al., 2002; Fig. 7A). In parallel, BiFC with all pairings of CP_{SP} and CP_{Po} confirmed the strong homologous reactions of CP_{SP}, and negligible interactions between CP_{SP} and CP_{Po}, or homologous reaction of CP_{Po} (Fig. 7A, and data not shown).

Silencing of NbBOR1 results in induction of necrosis at 25 °C by AltMV 3-7

Plants in which the boron transporter was silenced by VIGS using TRV:NbBOR1 showed significant reductions in NbBOR1 mRNA, estimated by Q-RTPCR at 35% of the level detected in plants infected with WT TRV (data not shown). At low temperature (ca. 15 °C), all plants challenged with AltMV 3-7 developed systemic necrosis (comparable to that seen in Fig. 6) whether preinfected with WT TRV or TRV:NbBOR1 (data not shown). However, at 25 °C plants preinfected with WT TRV developed only mosaic after challenge with AltMV 3-7, whereas plants silenced with TRV:NbBOR1 showed mosaic of the petiole and intraveinal necrosis of the leaf lamina following infection with AltMV 3-7 (Fig. 8, upper). In contrast, no necrosis was observed in plants inoculated with AltMV 3-$7_{Po\text{-}CP}$ at either temperature, regardless of whether NbBOR1 was silenced (Fig. 8, lower; and data not shown).

When plants in which NbBOR1 was silenced using TRV:NbBOR1 were challenged with PVX overexpressing either CP_{SP} or CP_{Po}, mosaic without necrosis was observed at 25 °C, with increased chlorosis in plants challenged with PVX-CP_{SP} (Supplemental Fig. 8), whereas at 15 °C necrosis was observed with PVX-CP_{SP} but not PVX-CP_{Po}; these results were similar to those previously observed in plants without prior TRV infection (Fig. 2; and data not shown).

Discussion

Here we have identified the CP of AltMV-SP as a pathogenicity determinant, and as the elicitor of a temperature-sensitive systemic necrosis (SN) in *N. benthamiana*. We have previously shown that SN was correlated with increased accumulation at 15 °C of four infectious clones each having the identical AltMV CP_{SP}, but differing in replication efficiency; and that exchange of the AltMV POL domain differing by three aa also resulted in increased accumulation and necrosis (Lim et al., 2010a). It is noteworthy that AltMV infectious clones 3-1 and 4-1 having lower accumulation levels induced limited necrosis at 15 °C, but did not kill plants by 30 dpi (Lim et al., 2010a). The SN induced by AltMV was similar to that caused by CaMV-W260 in *N. clevelandii*, a host response controlled by a single gene (Király et al., 1999). Although increased AltMV accumulation at 15 °C contributes to SN, substitution of CP_{Po} into AltMV 3-7 ablated necrosis at both 15 °C and 25 °C in

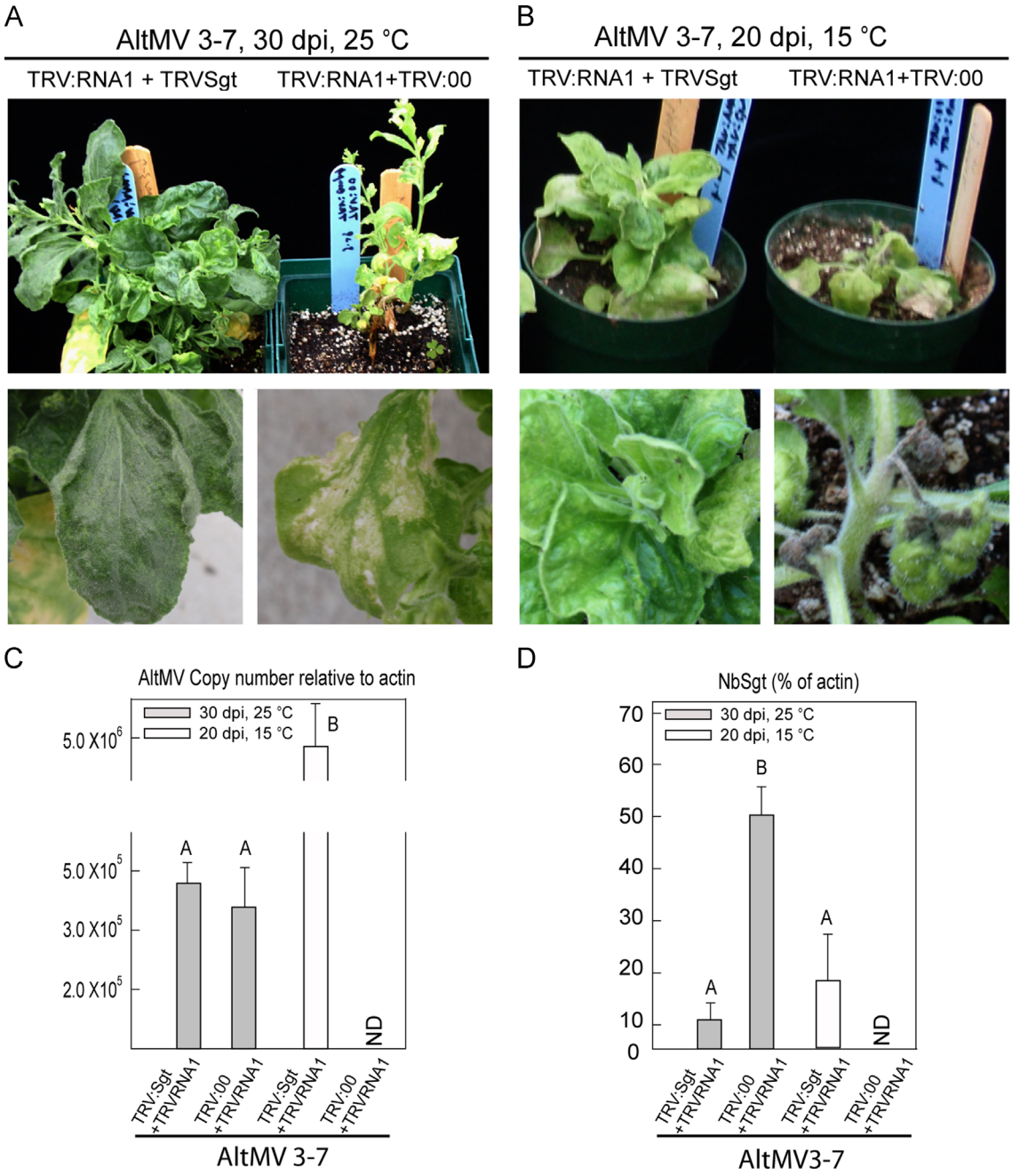

Fig. 5. Silencing of *SGT1* ablates systemic necrosis. *NbSGT1* was silenced in *N. benthamiana* using a TRV vector to analyze AltMV-induced systemic necrosis. Two-week old *N. benthamiana* were infiltrated with TRV carrying a fragment of *NbSGT1.1* (TRV:SGT), or the vector control (TRV:00), then 20 days later inoculated with 3-7 and placed (A) at 25 °C and (B) at 15 °C. Enlargements of AltMV-infected TRV:SGT and TRV:00 plants (lower) more clearly show the symptom differences. At 25 °C and 15 °C severe necrosis were detected only in TRV:00 plants, and these plants were almost killed at 15 °C by 20 dpi. (C and D) Q-RTPCR with AltMV CP-specific and *NbSGT1*-specific primers; ND=Not determined, as upper leaves of plants inoculated with TRV:00+TRV:RNA1 and AltMV were necrotic (see panel B), such that it was not possible to extract RNA. (C) AltMV copy number in *N. benthamiana* normalized to actin. (D) *NbSGT1* copy number normalized to actin. Results with the same letter were not significantly different ($P=0.05$).

N. benthamiana; levels of accumulation of 3-7 and 3-$7_{CP\text{-}Po}$ at each temperature were equivalent as shown by Q-RTPCR. In contrast, substitution of AltMV-Po TGB2/3 did not affect symptoms. Substitution of CP_{Po} also ameliorated symptoms in *A. dentata*, and allowed systemic infection of soybean with only mild symptoms. AltMV-induced necrosis can therefore be assigned to the differences between CP_{SP} and CP_{Po}, and not to differences in accumulation level as shown for SN in *N. benthamiana* infected with severe isolates of PlAMV (Komatsu et al., 2010, 2011) or with PVX (Park and Kim, 2012); indeed, induction of necrosis by the HEL elicitor domain of an 'asymptomatic' isolate of PlAMV was demonstrated by high level expression through agroinfiltration (Komatsu et al., 2011).

Whereas necrosis was induced following agroinfiltration of PVX CP into *Rx*-transgenic *N. benthamiana* (Bendahmane et al., 1999), or SN following agroinfiltration of CaMV-W260 gene VI into *N. clevelandii* or *Nicotiana edwardsonii* (Palanichelvam et al., 2000), or PlAMV RdRp or its helicase domain into *N. benthamiana*

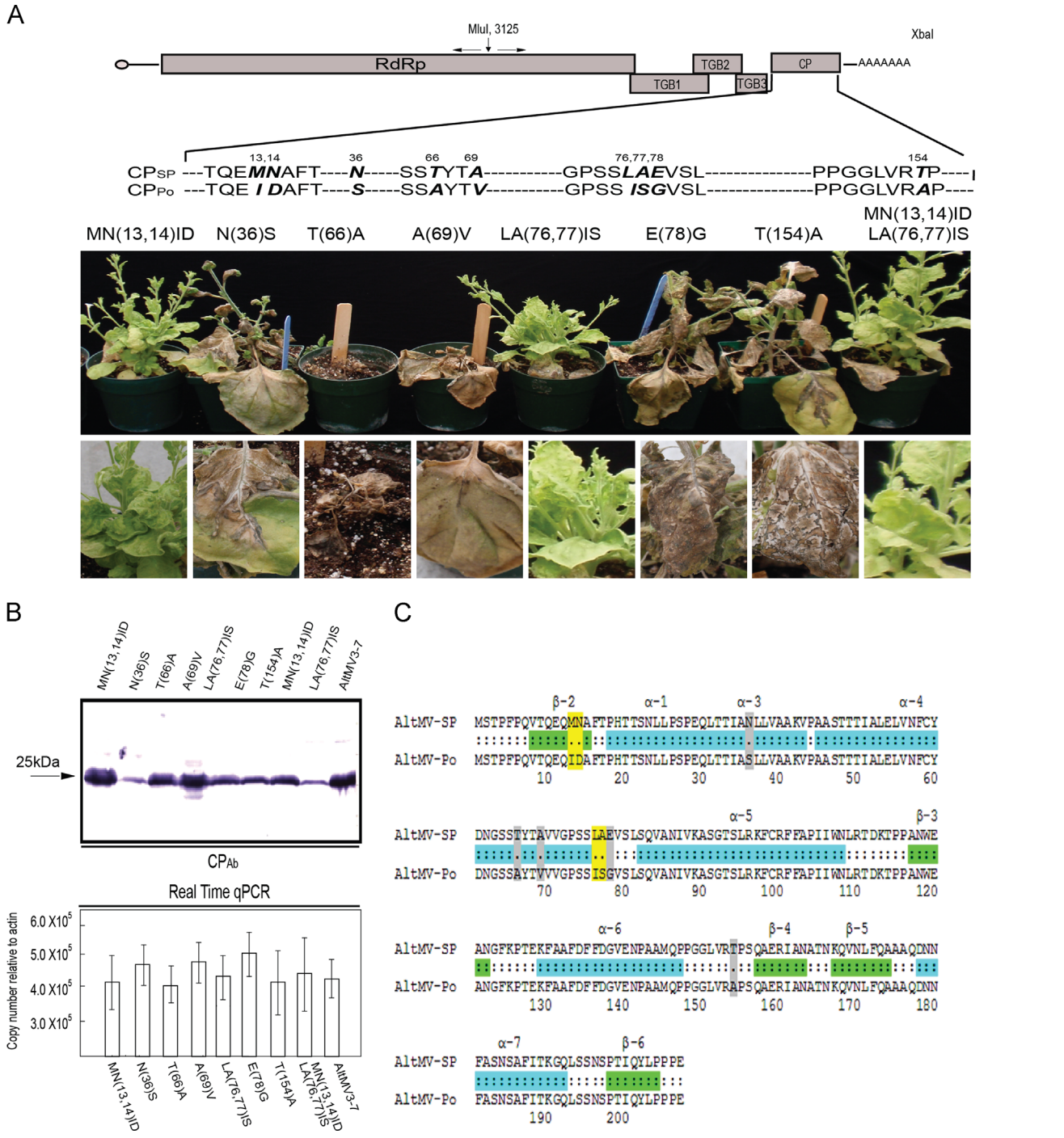

Fig. 6. Substitution of residues from AltMV-Po CP into AltMV 3-7. (A) Eight mutants [MN(13,14)ID, N(36)S, T(66)A, A(69)V, LA(76,77)IS, E(78)G, T(154)A, and MN(13,14)ID+LA(76,77)IS] were produced. RNA transcripts were inoculated at 15 °C. By 30 dpi all mutants except MN(13,14)ID, LA(76,77)IS, and MN(13,14)ID+LA(76,77)IS induced severe symptoms in *N. benthamiana*. (B) (Upper) Western blot of protein extracts from AltMV WT (3-7) and the CP mutants shown in (A), developed with AltMV-specific antibody; the migration of a 25 kDa marker protein is indicated; (lower) Q-RTPCR demonstrating that accumulation levels of the CP mutants was equivalent to that of AltMV 3-7; the average and SD of five replicate reactions are shown. Note that extracts were made from plants grown at 25 °C, prior to development of significant necrosis, and that the samples for the western blot were collected at a later time, from the same plants. (C) Alignment of aa sequences of AltMV-SP (3-7) and AltMV-Po CP, with differences highlighted; those in yellow were associated with necrosis. AltMV CP domains equivalent to predicted PVX α-helix and β-sheet domains are marked in blue and green, respectively; AltMV lacks the region equivalent to PVX α-2, and AltMV α-1 and α-3 equivalents are not separated. AltMV residues 13 and 14 fall within β-2, while residues 76 and 77 are between domains α-4 and α-5, predicted to be at the virion core (Dobrov et al., 2007).

(Komatsu et al., 2011), agroinfiltration of CP_{SP} did not induce necrosis despite inclusion of p19 in the agroinfiltrations to minimize potential silencing of the CP constructs and maximize expression. Similarly, transferring agroinfiltrated plants to 15 °C did not result in any apparent necrosis. However, overexpression of CP_{SP}, but not CP_{Po} from a PVX vector effectively induced SN, with greater necrosis at 15 °C than at 25 °C. Whereas it might be argued that necrosis was observed only from PVX expression because an additional potexviral protein is necessary for induction of necrosis, PVX expression of CP_{Po} did not induce any systemic

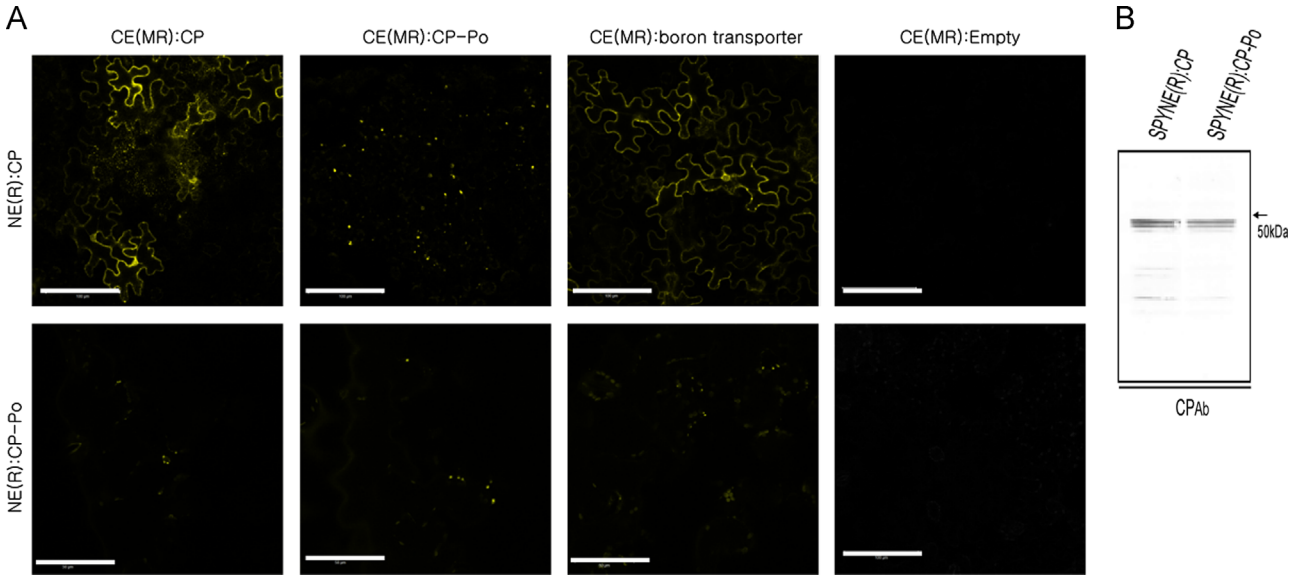

Fig. 7. Biomolecular fluorescence complementation assay. (A) CP_{SP} and CP_{Po} expressed in pSPYNE(R) to assay homologous and heterologous interactions with CP_{SP} and CP_{Po} cloned in pSPYCE(MR). In addition, the *N. benthamiana* boron transporter gene NbBOR1 was cloned in pSPYCE(MR), and assayed for interactions with CP_{SP} and CP_{Po} cloned in pSPYNE(R). LSCM was used to detect eYFP expression in epidermal layer at 2 days after agroinfiltration. NE(R):CP=pSPYNE(R):CP_{SP}; NE(R):CP-Po=pSPYNE(R):CP_{Po}; CE(MR):CP=pSPYCE(MR):CP_{SP}; CE(MR):CP-Po=pSPYCE(MR):CP_{Po}; CE(MR):boron transporter=pSPYCE(MR):NbBOR1; CE(MR):Empty=pSPYCE(MR) without insert. Bar=200 um. (B) Western blot of *N. benthamiana* leaves agroinfiltrated with pSPYNE(R):CP or pSPYNE(R):CP_{Po}, and developed with AltMV-specific antibody; the migration of a 50 kDa marker protein is indicated.

necrosis even at 15 °C. This confirmed the ability of CP_{SP} to function as an elicitor of systemic necrosis, and the temperature sensitivity of the interaction. This experiment also demonstrated the requirement for a high concentration of CP to induce necrosis, as expression from PVX resulted in an estimated 200-fold increase of AltMV CP expression over agroinfiltration. It is also notable that Komatsu et al. (2011) reported that the HEL elicitor of a normally asymptomatic isolate of PlAMV could induce SN when expressed at high levels by agroinfiltration, suggesting that elicitor concentration is very important for induction of SN.

It should be noted that agroinfiltration results only in local expression of CP_{SP} or CP_{Po}, whereas PVX expression causes SN without obvious local necrosis. Similarly, SN with PVX expression develops only about 2 weeks after infection, while at 2 weeks after agroinfiltration leaves were typically chlorotic and starting to collapse even in controls infiltrated with the empty pGD vector. We have previously shown that AltMV accumulation at 15 °C was approximately four- to five-fold that at 25 °C (Fig. 1C; Lim et al., 2010a), whereas no such increase in CP expression was observed at 15 °C compared to 25 °C after agroinfiltration.

The SN response to CP_{SP} differs from the typical expectation of an elicitor/viral *avr* gene; in most cases elicitors induce a hypersensitive response (HR), or as with the *Rx* gene for PVX resistance, an extreme local resistance at the inoculation site, preventing systemic infection (e.g. Bendahmane et al., 1999; Bonas and Lahaye, 2002). Most instances of sHR correlate with *R* gene-mediated local HR against the same or closely-related virus isolates (Dinesh-Kumar et al., 2000; Hajimorad et al., 2005). The *Rx* gene was originally described as specific for PVX but has more recently been shown to confer resistance against other potexviruses in both *N. benthamiana* (Baurès et al., 2008) and tomato (Candresse et al., 2010). Our experiments demonstrate that *Rx* has no effect on systemic spread or symptoms of either AltMV 3-7 or 3-$7_{Po\text{-}CP}$, suggesting that unlike the other non-PVX potexviruses *Narcissus mosaic virus* (NMV), *White clover mosaic virus*, *Cymbidium mosaic virus*, and *Pepino mosaic virus* (PepMV; Baurès et al., 2008; Candresse et al., 2010), AltMV is not an elicitor of *Rx*. However, ablation of necrosis in *N. benthamiana* by VIGS of *SGT1* demonstrates that necrosis is dependent on another R gene or similar resistance gene, as *SGT1* has previously been shown to be necessary for the function of Rx and other NBS–LRR proteins (e.g. Azevedo et al., 2006; Komatsu et al., 2011; Peart et al., 2002) and also for non-host resistance (Peart et al., 2002). It has also been noted that not only *SGT1*, *Hsp90*, *Rar1*, *RanGap1*, and *RanGap2* are necessary for Rx function, but that at least five other independent host factors mediate the resistance, possibly by affecting recognition of the PVX CP elicitor of Rx or the intensity of the Rx response (Sturbois et al., 2012). Host factors may therefore modulate the specificity or intensity of recognition of the pathogen elicitor (Baurès et al., 2008; Sturbois et al., 2012). It is therefore reasonable to propose that NbBOR1, which we show here to interact differentially with CP_{SP} and CP_{Po}, may be such a host factor modulating the SN response to AltMV (see below).

Mitogen-activated protein kinase (MAPK) cascades respond to stresses induced by both abiotic and biotic factors (Rodriguez et al., 2010), and many MAPK kinase kinases (MAPKKKs) are involved in programmed cell death and stress or defense responses, including HR such as the *N*-gene response to TMV (Jin et al., 2002). Silencing of specific MAPKK and MAPK genes in tobacco attenuates HR against TMV mediated by *N* (Jin et al., 2003). Both PlAMV-induced SN and *Rx*-mediated HR against PVX involve a signaling cascade leading to cell death (Komatsu et al., 2010). Three non-redundant MAPKKK genes are positive regulators of PlAMV-induced necrosis, and as many as four distinct MAPK cascades are coordinately involved in plant cell death (Hashimoto et al., 2012). The different *N. benthamiana* MAPKKKs differed considerably in the level of expression required to induce complete cell death (Hashimoto et al., 2012). As MAPK cascades are involved in a broad range of plant responses, it is possible that CP_{SP} either interacts inefficiently or only indirectly with one of the MAPKKKs that must itself accumulate to a higher level to induce cell death.

We further examined the elicitor function of CP_{SP} by amino acid exchanges between CP_{SP} and CP_{Po}. Two mutants, MN(13,14)ID and

Fig. 8. Effects of NbBOR1 silencing on symptom development in plants challenged with AltMV 3-7 and AltMV 3-7$_{Po\text{-}CP}$. Plants of *N. benthamiana* were infected with WT TRV (left) or TRV:NbBOR1 (right) at the four-leaf stage, and 20 days later inoculated with transcripts of AltMV 3-7 (upper) or AltMV 3-7$_{Po\text{-}CP}$ (lower) and grown at 25 °C. Plants preinfected with WT TRV developed mosaic when challenged with either AltMV 3-7 (upper left) or AltMV 3-7$_{Po\text{-}CP}$ (lower left), whereas only plants challenged with AltMV 3-7 developed necrosis of the petiole and intraveinally in the leaf laminar (upper right and details in center panels). Q-RTPCR showed that the level of NbBOR1 mRNA in the silenced plants was c.35% of the level in plants infected by control WT TRV (data not shown).

LA(76,77)IS in different regions of the CP, as well as the combined mutant MN(13,14)ID+LA(76,77)IS, resulted in ablation of necrosis even at 15 °C, whereas five additional mutants did not. Collectively these mutants substitute all of the nine aa differences between CP_{SP} and CP_{Po}. By comparison to the structures predicted for PVX (Baratova et al., 2004; Dobrov et al., 2007) and PapMV CP (Yang et al., 2012), N-terminal domain mutant MN(13,14)ID affects surface-exposed residues. The structure of Yang et al. (2012) shows the N-terminal region of PapMV CP including residue F13 overlapping and interacting with a hydrophobic pocket on the exterior surface of the adjacent subunit, consistent with F13 being critical for PapMV particle formation (Laliberté Gagné et al., 2008), and the 'scaffold' role of the N-terminal domain of PVX (Lukashina et al., 2012). However, even PapMV mutants with substitutions for F13 were able to form multisubunit aggregates, while residues K97 and E128 affect both RNA binding and self assembly of subunits, indicating that other domains of the CP have a major influence on subunit:subunit interactions (Laliberté Gagné et al., 2008; Tremblay et al., 2006).

It is notable that residues MN(13,14) and LA(76,77), found necessary for induction of SN at 15 °C, appear to be located on subunit surfaces within the same turn of the virion helix (Supplemental Fig. 7); all other differential residues except E(78)G and N(36)S are on surfaces between turns of the helix according to the structure predicted by Yang et al. (2012) for PapMV, the potexvirus most closely related to AltMV (Geering and Thomas, 1999; Hammond et al., 2006a). E(78)G has a similar location and predicted secondary structure to LA(76,77)IS, but did not ablate necrosis; E(78)G is also predicted to have the most extreme change in CP pI. Yeast two-hybrid analysis differentiated MN(13,14)ID and LA(76,77)IS; the former had strong self-interactions, and LA(76,77)IS weak interactions similar to CP_{Po} (Table 2). Neither pI nor elicitor strength were correlated with self-interaction in the yeast two-hybrid system, or with necrosis..

We note that the three-dimensional reconstruction of PapMV of Yang et al. (2012) suggests a structure with approximately 10 subunits per turn of the virion helix. This differs from the prediction of slightly less than nine subunits per turn for not only PapMV, but also for PVX and NMV, obtained by Kendall et al. (2013) by a different combination of methods. Earlier work had suggested relatively dense axial intersubunit contacts at low radius, and relative sparse contacts at high radius, leading to the flexuous nature of PapMV virions (Erickson et al., 1983). Our results indicate that none of the residues that differ between CP_{SP} and CP_{Po} are critical for particle assembly or virion stability, and have no significant effect on particle flexibility, but that several significantly affect symptom expression, potentially through interactions with a host *R* gene to induce SN under low temperature conditions.

Both MN(13,14)ID and LA(76,77)IS may influence secondary or three-dimensional structure of the AltMV CP in a way that affects the interactions between CP and one or more host proteins involved in the recognition of CP as an elicitor protein. Baurès et al. (2008) and Candresse et al. (2010) have noted that there are relatively low levels of aa sequence identity in the elicitor domains of the potexviruses interacting with Rx, and that conservation of structural elements is more important than a specific aa sequence. Although two specific CP residues (K121 and R127) are required for PVX to overcome Rx-mediated resistance (Goulden et al., 1993), mutation of only the more typical T121K induces predicted conformational changes in the PVX CP (Querci et al., 1993). In contrast, many individual aa mutations between residues 41 and 125 of the PepMV CP allowed escape from restriction in *Rx*-transgenic tomato (Candresse et al., 2010).

Although the yeast two-hybrid interactions clearly differentiated subunit interaction strength of CP_{Po} and LA(76,77)IS (weak interactions) from CP_{SP} and the other CP mutants, these results must be interpreted cautiously, potentially reflecting the efficiency of CP multimerization in the absence of RNA and virion formation. CP_{SP}, but not CP_{Po}, yielded obvious dimers *in vivo* that were detected in a non-denaturing gel system, formed larger aggregates *in vivo* when coexpressed with GFP:CP, and formed dimers as a GST:CP fusion; BiFC also revealed obvious homologous interaction of CP_{SP} but not CP_{Po}. In contrast, TMV CP mutants with greatest elicitor strength were inhibited in aggregation to form disks and rods under conditions in which non-elicitors readily formed aggregates (Culver et al., 1994). Either the size distribution or lifetime of small TMV CP aggregates affects the ability to elicit the *N′* gene response, and CP aggregation state is affected by factors including temperature (Toedt et al., 1999). This may reflect the difference between a strong elicitor of HR, and an elicitor of SN that may have low affinity for the receptor (Bendahmane et al.,

1999), or for which differential interactions with a host factor may modulate the SN response (see below). Our results differ from those with TMV in that AltMV-SP, AltMV-Po, and all of the mutants examined are able to form virions and spread systemically at 15 °C and 25 °C.

In contrast to our results suggesting that CP_{Po} has weak self-interactions, it is of interest to note that Mukhamedzhanova et al. (2011) reported that CP of portulaca isolate AltMV-MU can form RNA-free virus-like particles (VLPs) *in vitro*, and formed filamentous VLPs at pH 8.0 as well as at pH 4.0. As the closely related PapMV CP forms filamentous VLPs at pH 4.0, but only 'small 13–33 S aggregates' at pH 8.0 (Erickson et al., 1976), this implies that AltMV-MU CP forms strong CP:CP interactions. The CP of AltMV-MU differs from that of AltMV-Po by only a single residue (I106M), which is unlikely to explain the differences observed between our results and those of Mukhamedzhanova et al. (2011).

Interestingly, Y2H data showed there is differential binding activity between CP_{SP} or CP_{Po} and the Arabidopsis boron transporter AtBOR1, confirmed by BiFC with the *N. benthamiana* homolog, NbBOR1. AtBOR1 has been reported to localize to the plasma membrane, especially in roots, and to effect xylem loading with boron in order to regulate boron concentration and protect shoots from boron deficiency (Takano et al., 2002). Either Boron (B) deficiency or excess can cause severe plant damage including the induction of necrosis (Cakmak and Römheld, 1997; Nable et al., 1997), and the concentration range between deficiency and toxicity is narrow (Takano et al., 2005). AtBOR1 is normally closely regulated by transport via endosomes to the vacuole for degradation when B is available in excess (Takano et al., 2005). It is possible that interaction with CP_{SP} interferes with BOR1 regulation. Whereas excess B typically results in necrosis at the leaf margin (Nable et al., 1997), B deficiency can also result in necrosis through a variety of effects including enhanced accumulation of phenols, excessive production of quinones and generation of toxic O_2 species (superoxide radicals, hydrogen peroxide, and hydroxyl radicals), and decreased production of ascorbic acid, SH-compounds, and glutathione reductase (Cakmak and Römheld, 1997). In addition to being involved in cell wall cross-linking, B is also reported to have direct structural functions in membranes, possibly by cross-linking glycoproteins (Wimmer et al., 2009), and it is notable that AtBOR1 is known to localize to the plasma membrane (Takano et al., 2002). Silencing of NbBOR1 by VIGS resulted in induction of necrosis by AltMV 3-7 at 25 °C that was not observed in control plants preinfected with the WT TRV, whereas no effect of NbBOR1 silencing was observed in plants infected with AltMV $3\text{-}7_{Po\text{-}CP}$ at either temperature (no necrosis). These results further suggest that only CP_{SP} can induce necrosis, primarily at low temperature, and that interaction of CP_{SP} with NbBOR1 inhibits the induction of necrosis at 25 °C. NbBOR1 may thus be a host factor modulating the temperature-sensitive SN response to AltMV. We will conduct further experiments to quantify B and elucidate the nature of the interaction between CP_{SP} and NbBOR1 resulting in induction of SN at low temperature, including possible involvement in a MAPK cascade affecting an *R* gene.

We cannot yet differentiate between the possibilities that (i) the aggregation state of AltMV CP_{SP} is affected by temperature as for TMV (Toedt et al., 1999); (ii) increased replication at 15 °C sufficiently increases abundance of a weak elicitor to induce systemic necrosis; or (iii) the host *R* gene response itself is temperature sensitive, as suggested for the TMV/*N* gene interaction (Padgett et al., 1997). The interactions of the host protein BOR1 and CP will be further investigated, which may make it possible to better explain the function of CP in the induction of necrosis, and to determine whether BOR1 is a host factor modulating CP recognition.

Materials and methods

Plant material

Seedlings of *N. benthamiana* were grown in 10 cm pots in a greenhouse. *Rx*-18 transgenic *N. benthamiana* (Bendahmane et al., 1999) was a gift from Peter Moffett (Boyce Thompson Institute) and were grown under the same conditions. Three- to four-week-old *N. benthamiana* plants were used for virus infection and agroinfiltration. Soybean (*Glycine max*) cv. Jack was grown in a greenhouse at 25 °C. *A. dentata* 'Purple Knight' was raised from seed and propagated by cuttings. Inoculated plants were grown in greenhouses maintained at 15 °C or 25 °C under a 14 h light regime.

Virus isolates and construction of AltMV infectious clones

All primers utilized in these experiments are shown in Supplemental Table 1. AltMV-SP was isolated from *Phlox stolonifera* cv. Sherwood Purple and maintained in *N. benthamiana* (Hammond et al., 2006a). Infectious clone AltMV 3-7 (Lim et al., 2010a) forms the basis of this work. Introduction of a multiple cloning site (MCS) has been described (Lim et al., 2010a). Young *N. benthamiana* plants were inoculated with *in vitro* transcripts (see below; two leaves per plant, three plants per transcribed clone). Inoculated plants were tested by RTPCR as necessary using AltMV-specific primers PP12 and PP15. AltMV-Po was isolated from *Portulaca grandiflora*, and maintained in *N. benthamiana*; cloning of the 3′ region has been reported previously (Hammond et al., 2006a).

PVX infectious clones expressing AltMV-SP or AltMV-Po CP

A full-length PVX (isolate UK3) PCR product derived from plants inoculated with pP2CS (Baulcombe et al., 1995) transcripts was ligated into the TOPO vector (Invitrogen), and a modified MCS was then inserted, creating pPVX-MCS (Lim et al., 2010b). The CP genes of AltMV-SP and AltMV-Po were separately amplified and inserted into pPVX-MCS, creating pPVX-CP_{SP}, and pPVX-CP_{Po} respectively.

In vitro transcription reactions and plant inoculations

Full-length AltMV cDNA clones were linearized with *Xba*I, and transcript RNA generated using T7 RNA polymerase as described (Petty et al., 1989). PVX cDNA clones were linearized with *Spe*I, and similarly transcribed. Transcribed RNAs were ethanol precipitated and resuspended in 20 μl of GKP buffer (50 mM glycine, 30 mM KHPO4, pH 9.2, 1% bentonite, 1% celite) per 50 μl transcription reaction and 10 μl used per leaf to inoculate two leaves per plant of *N. benthamiana* (Petty et al., 1989).

Quantitative real-time reverse transcription PCR (Q-RTPCR)

Total RNA was isolated from *N. benthamiana* using the RNeasy Mini Kit (Qiagen), and treated with DNase I following the manufacturer's recommendation; 2 μg total RNA was used to generate cDNA in 20 μl reactions using SuperScript III RNase H^- Reverse Transcriptase (Invitrogen) with 0.5 μg of $oligo(dT)_{20}$ primer. Q-RTPCR was performed with selected primer sets (Supplemental Table 1) as described (Bae et al., 2006). Relative transcript levels of each target (AltMV CP, *NbSGT1.2* [AF516181], and *NbBOR1* [KC631823]) were normalized with respect to *N. benthamiana* actin (AY179605) transcript levels (relative to actin), which is a constitutively expressed gene. Mean values were calculated from four individual plant replications, and results compared by ANOVA.

Construction of AltMV 3-7$_{Po\text{-}TGB2/3}$, AltMV 3-7$_{Po\text{-}CP}$, and CP mutants

The AltMV-Po TGB2/3 region was amplified using primers Po-TGB2-F/Po-TGB2-R, digested with *Xma*I and *Bam*HI and substituted for the equivalent TGB2/3 region of AltMV 3-7, creating AltMV 3-7$_{TGB23\text{-}Po}$. The CP gene and 3′ UTR of AltMV-Po was amplified using primers Po-CP-F and XbaI-R2, and substituted into pAltMV:MCS (Lim et al., 2010a); the *Xma*I/*Xba*I fragment of pAltMV:MCS:Po-CP was then substituted into full-length clone 3-7 to form AltMV 3-7$_{Po\text{-}CP}$. Selected residues of the AltMV 3-7 CP were mutated to residues present in AltMV-Po by overlap PCR (Wurch et al., 1998), creating CP mutants MN(13,14)ID, N(36)S, T(66)A, A(69)V, LA(76,77)IS, E(78)G, T(154)A, and MN(13,14)ID+LA(76,77).

Agrobacterium infiltration, AltMV constructs, and subcellular localization

All binary vectors used were derived from pGD or pGDG as previously described (Goodin et al., 2002). CP$_{SP}$ and CP$_{Po}$ were amplified from AltMV 3-7 and AltMV-Po respectively, and inserted to the *Xho*I and *Bam*HI sites of pGD.

A. tumefaciens EHA105 was separately transformed with each pGD-derived construct; colonies were scraped from fresh plates and diluted to approximately OD_{600}=0.4 in infiltration buffer (10 mM MES pH 5.6, 10 mM $MgCl_2$) containing 150 μM 3′,5′-dimethoxy-4′-hydroxyacetophenone (Aldrich). When more than one culture was used for coagroinfiltration, each culture was diluted to OD_{600}=0.4 before adding to the mixture. Bacteria were then incubated at room temperature for 2–3 h before infiltration with a 1-cc syringe at the underside of the leaf. Agrobacteria containing pGD:p19 (a gift of Andy Jackson; Lim et al., 2010a) were included at 0.1 volume of all agroinfiltration mixes for CP expression to minimize silencing and maximize expression.

Plants of *N. benthamiana* infiltrated with pGD:CP$_{SP}$, pGD:CP$_{Po}$, or pGD (empty vector) were either maintained in a growth chamber at 22 °C, or transferred after 24 h in the growth chamber either to a greenhouse maintained at a nominal 25 °C or an air-conditioned greenhouse at a nominal 15 °C.

Virus-induced gene silencing (VIGS).

The TRV:00 VIGS vector (Ratcliff et al., 2001; Peart et al., 2002), TRV:SGT (Peart et al., 2002), and TRV:Sulfur (containing the *N. benthamiana* homolog of the tobacco sulfur gene (Fitzmaurice et al., 1999)) were gifts from Peter Moffett (Boyce Thompson Institute).

A 253 bp fragment of the *N. benthamiana* boron transporter gene (*NbBOR1*) was amplified from *N. benthamiana* cDNA using primers based on the GenBank sequence (KC631823) to insert into TRV RNA2 (Dinesh-Kumar et al., 2003). This TRV:NbBOR1 VIGS construct was transformed into *Agrobacterium tumefaciens* GV3101.

N. benthamiana plants at the four leaf stage (2 weeks old) were infiltrated with *A. tumefaciens* containing WT TRV or TRV VIGS constructs respectively (Dinesh-Kumar et al., 2003). Where appropriate, plants were subsequently inoculated with transcripts of AltMV 3-7, AltMV 3-7$_{Po\text{-}CP}$, PVX-CP$_{SP}$. or PVX-CP$_{Po}$, at 20 days after agroinfiltration of TMV, when silencing was established.

Yeast two-hybrid assays to examine CP:CP interactions

Yeast two-hybrid vectors (James et al., 1996), were designed to produce fusions of the Gal4 activation domain (AD) or the Gal4 binding domain (BD) to the N-terminus of the proteins to be tested for interactions. To construct fusions to the AD (pGAD:CP$_{SP}$, pGAD:CP$_{Po}$, pGAD:CP$_{MN(13,14)ID}$, pGAD:CP$_{N(36)S}$, pGAD:CP$_{T(66)A}$, pGAD:CP$_{A(69)V}$, pGAD:CP$_{LA(76,77)IS}$, pGAD:CP$_{E(78)G}$, pGAD:CP$_{T(154)A}$) and the BD (pGBDU:CP$_{SP}$, pGBDU:CP$_{Po}$, pGBDU:CP$_{MN(13,14)ID}$, pGBDU:CP$_{N(36)S}$, pGBDU:CP$_{T(66)A}$, pGBDU:CP$_{A(69)V}$, pGBDU:CP$_{LA(76,77)IS}$, pGBDU:CP$_{E(78)G}$, and pGBDU:CP$_{T(154)A}$), CP sequences were amplified and introduced between the *Eco*RI and *Bam*HI sites of pGDBU and pGAD. Yeast strain PJ69-4A was transformed with *LEU2*-selected AD and *URA3*-selected BD constructs and selected, and colonies were tested for interactions as previously described (Becker et al., 1991; Lim et al., 2010a).

Affinity chromatography

For GST pull-down experiments, two proteins (with one fused to pGD-GST) were coexpressed in *N. benthamiana* through agroinfiltration as described by Deng et al. (2007). CP$_{SP}$ and CP$_{Po}$ were each amplified using primers Coat XhoI-F/Coat BamHI-R. Each PCR product was cloned between the *Xho*I and *Bam*HI sites of pGD-GST and pGD vectors. At 2 days post-infiltration, 3 g of leaf tissue was macerated with 4 ml of STE buffer (10 mM Tris–HCl, pH 8.0, 150 mM NaCl, 1 mM EDTA) containing 2% bovine serum albumin, 10% glycerol, 1.0 mM phenylmethanesulfonyl fluoride, and 0.1 μg/ml each of antipain, leupeptin, and pepstatin (Sigma). After 3 h of incubation of the extract at 4 °C with 100 μl of glutathione–Sepharose 4B slurry (GE Healthcare Life Sciences) diluted 1:1 with PBS, the GST fusions and bound coat proteins were purified by elution with 100 μl reduced glutathione according to the manufacturer's instructions. Eluted proteins were assessed in 10% SDS-polyacrylamide gels as described (Deng et al., 2007).

Electrophoresis and western blotting

Extracts of infected or agroinfiltrated leaves were made in CellLytic P Cell Lysis buffer (Sigma) either with (for SDS-PAGE) or without 10 mM β-mercaptoethanol (for non-denaturing PAGE), and proteins separated on 10% or 12% polyacrylamide (non-denaturing) or SDS-polyacrylamide gels.

AltMV infections were confirmed as necessary using western blotting using a 1:2000 dilution of AltMV-specific antibody (a gift from Andrew Geering; Geering and Thomas, 1999; Hammond et al., 2006a); GFP fusion proteins were detected using the Anti-GFP Living Colors monoclonal antibody (Clontech) as recommended by the manufacturer. Expression of GST fusion proteins was verified using a 1:5000 dilution of anti-GST antibody (Sigma). Detection was with 1:2500 diluted alkaline phosphate-conjugated goat anti-rabbit or goat anti-mouse antibody (Kirkegaard & Perry) and NBT:BCIP substrate (Sigma).

Detection of fluorescence in N. benthamiana epidermal cells

Fluorescence in epidermal cells of *N. benthamiana* leaves was visualized by laser scanning confocal microscopy (LSCM) using a Zeiss LSM 710 microscope (Carl Zeiss MicroImaging, Inc.). An Argon laser was used to excite GFP at 488 nm and emission detected between 500 and 520 nm (Lim et al., 2010a). For detection of eYFP, excitation was at 488 nm, and emission was detected between 492 and 598 nm.

Sequence analysis

The predicted effects of mutations on CP structure, hydropathy, and isoelectric point were evaluated using programs PELE, GREASE, and PI in the Molecular Biology Workbench suite (http://workbench.sdsc.edu/). Predicted protein:protein interactions were examined using ProSite (Bairoch et al., 1997) at the PredictProtein server (http://www.predictprotein.org/). The AltMV

CP was aligned (ALIGN) with that of PVX (M38460) in order to identify the equivalents of the α-helix and β-sheet domains identified by Dobrov et al. (2007).

The AltMV CP structure was overlaid upon the three dimensional structure (Protein Data Bank accession 4DOX) determined for the closely-related PapMV by Yang et al. (2012), using the Cn3D program available through NCBI (http://www.ncbi.nlm.nih.gov/Structure/CN3D/cn3d.shtml).

Yeast two-hybrid assays to identify CP:host protein interactions from an Arabidopsis cDNA library

The AltMV CP gene was cloned into pGBKT7 at *Eco*RI and *Bam*HI sites, in fusion with the Gal4 DNA-BD, and the resulting plasmid (pGBKT-CP) was used to transform yeast competent cells (strain AH109) for bait protein expression. *A. thaliana* cDNA library (CD4-30, Arabidopsis Biological Resource Center, http://www.abrc.osu.edu) in pAD-GAL4-2.1 (in fusion with Gal4 DNA-AD) plasmid was used to transform yeast competent cells containing pGBKT-CP. Transformant cells were screened on SD agar His-, Leu-, Trp-plus Aureobasidin A. Yeast colonies obtained were grown on the same media including the chromogenic substrate X-α-galactosidase; only colonies developing blue color were considered positive. *A. thaliana* genes encoding proteins involved in binding AltMV CP were amplified from each selected yeast colony using appropriate primers, sequenced, and identified using BLASTn at NCBI. The *N. benthamiana* homolog *NtBOR1* of the identified *AtBOR1* boron transporter gene (deposited in GenBank as KC631823) was amplified using primers (Supplemental Table 1) designed from sequences conserved between the *N. tabacum* (EU599083) and *Solanum lycopersicum* (EU591593; AK320292) homologs, and a tagged poly(T) reverse primer. The NbBOR1 coding region was then amplified with specific primers pSPY-NbBor1-F2/pSPY-NbBor1-R (Supplemental Table 1) including appropriate restriction sites to clone into pSPYNE173 (see below).

Bimolecular fluorescence complementation (BiFC)

The AltMV CP and CP-Po genes were subcloned into both pSPYCE(M) and pSPYNE173, and the NbBOR1 boron transporter was subcloned into pSPYNE173, as translational fusions with either the C- (pSPYCE(M)) or the N-terminal (pSPYNE173) sequence of the eYFP gene (Waadt et al., 2008). Empty pSPYCE (M) and pSPYNE173 were included as negative controls. Constructs were agroinfiltrated as previously described and eYFP fluorescence was observed at 3 dpa by LSCM. Expression of the BiFC CP constructs was assessed by western blotting using AltMV-specific antibody as described above.

Electron microscopy

Virus particles of AltMV-SP, AltMV 3-7, AltMV-Po, and AltMV CP mutants in leaf dips or partially purified preparations were stained with sodium phosphotungstic acid, pH 7.0, and examined either in a Leo Electron LEO 902A electron microscope, or a JEOL 100CX II electron microscope equipped with an HR digital camera system (Advanced Microscopy Techniques Corp., Woburn, MA).

Acknowledgments

We thank Michael Reinsel for the excellent technical support, and Margaret Dienelt for electron microscopy. We also thank Bob Owens, Les Domier, and two anonymous reviewers for useful suggestions. This work was supported by a grant from the National Research Foundation of Korea (NRF no. 2013R1A1A2007417), Republic of Korea.

Appendix. Supplemenary information

Supplementary data associated with this article can be found in the online version at http://dx.doi.org/10.1016/j.virol.2014.01.021.

References

Azevedo, C., Sadanandom, A., Kitagawa, K., Freialdenhoven, A., Shirasu, K., Schulze-Lefert, P., 2002. The RAR1 interactor SGT1, an essential component of R gene-triggered disease resistance. Science 295, 2073–2076.

Azevedo, C., Betsuyaku, S., Peart, J., Takahashi, A., Noël, L., Sadanandom, A., Casais, C., Parker, J., Shirasu, K., 2006. Role of SGT1 in resistance protein accumulation in plant immunity. EMBO J. 25, 2007–2016.

Bae, H., Kim, M.S., Sicher, R.C., Bae, H.J., Bailey, B.A., 2006. Necrosis- and ethylene-inducing peptide from *Fusarium oxysporum* induces a complex cascade of transcripts associated with signal transduction and cell death in *Arabidopsis*. Plant Physiol. 141, 1056–1067.

Bairoch, A., Bucher, P., Hofmann, K., 1997. The PROSITE database, its status in 1997. Nucleic Acids Res. 25, 217–221.

Baker, C.A., Breman, L., Jones, L., 2006. *Alternathera mosaic virus* found in *Scutellaria*, *Crossandra*, and *Portulaca* spp, in Florida. Plant Dis. 90, 833.

Baratova, L.A., Fedorova, N.V., Dobrov, E.N., Lukashina, E.V., Kharlanov, A.N., Nasonov, V.V., Serebryakova, M.V., Kozlovsky, S.V., Zayakina, O.V., Rodionova, N.P., 2004. N-terminal segment of *Potato virus X* coat protein subunits is glycosylated and mediates formation of a bound water shell on the virion surface. Eur. J. Biochem. 271, 3136–3145.

Baulcombe, D.C., Chapman, S., Santa Cruz, S., 1995. Jellyfish green fluorescent protein as a reporter for virus infections. Plant J. 7, 1045–1053.

Baurès, I., Candresse, T., Leveau, A., Bendahmane, A., Sturbois, B., 2008. The Rx gene confers resistance to a range of potexviruses in transgenic *Nicotiana* plants. Mol. Plant–Microbe Interact. 21, 1154–1164.

Becker, D.M., Fikes, J.D., Guarente, L., 1991. A cDNA encoding a human CCAAT-binding protein cloned by functional complementation in yeast. Proc. Natl. Acad. Sci. USA 88, 1968–1972.

Bendahmane, A., Kohm, B.A., Dedi, C., Baulcombe, D.C., 1995. The coat protein of *Potato virus X* is a strain-specific elicitor of Rx1-mediated virus resistance in potato. Plant J. 8, 933–941.

Bendahmane, A., Kanyuka, K., Baulcombe, D.C., 1999. The Rx gene from potato controls separate virus resistance and cell death responses. Plant Cell 11, 781–792.

Bhattacharjee, S., Zamora, A., Azhar, M.T., Sacco, M.A., Lambert, L.H., Moffett, P., 2009. Virus resistance induced by NB-LRR proteins involves Argonaute4-dependent translational control. Plant J. 58, 940–951.

Bonas, U., Lahaye, T., 2002. Plant disease resistance triggered by pathogen-derived molecules: refined models of specific recognition. Curr. Opin. Microbiol. 5, 44–50.

Cakmak, I., Römheld, V., 1997. Boron-deficiency induced impairments of cellular functions in plants. Plant Soil 193, 71–83.

Candresse, T., Marais, A., Faure, C., Dubrana, M.P., Gombert, J., Bendahmane, A., 2010. Multiple coat protein mutations abolish recognition of Pepino mosaic potexvirus (PepMV) by the potato Rx resistance gene in transgenic tomatoes. Mol. Plant–Microbe Interact. 23, 376–383.

Ciuffo, M., Turina, M., 2004. A potexvirus related to *Papaya mosaic virus* isolated from moss rose (*Portulaca grandiflora*) in Italy. Plant Pathol. 53, 515.

Culver, J.N., Stubbs, G., Dawson, W.O., 1994. Structure–function relationship between *Tobacco mosaic virus* coat protein and hypersensitivity in *Nicotiana sylvestris*. J. Mol. Biol. 242, 130–138.

Deng, M., Bragg, J.N., Ruzin, S., Schichnes, D., King, D., Goodin, M.M., Jackson, A.O., 2007. Role of the *Sonchus yellow net virus* N protein in formation of nuclear viroplasms. J. Virol. 81, 5362–5374.

Dinesh-Kumar, S.P., Tham, W.H., Baker, B.J., 2000. Structure–function analysis of the *Tobacco mosaic virus* resistance gene *N*. Proc. Natl. Acad. Sci. USA 97, 14789–14794.

Dinesh-Kumar, S.P., Anandalakshmi, R., Marathe, R., Schiff, M., Liu, Y., 2003. Virus-induced gene silencing. Methods Mol. Biol. 236, 287–294.

Dobrov, E.N., Nemykh, M.A., Lukashina, E.V., Baratova, L.A., Drachev, V.A., Efimov, A.V., 2007. Modified model of the structure of the *Potato virus X* coat protein. Mol. Biol. 41, 638–641.

Erickson, J.W., Bancroft, J.B., Horne, R.W., 1976. The assembly of *Papaya mosaic virus* protein. Virology 72, 514–517.

Erickson, J.W., Hallett, F.R., Bancroft, J.B., 1983. Subassembly aggregates of papaya mosaic virus protein. Virology 129, 207–211.

Fitzmaurice, W.P., Nguyen, L.V., Wernsman, E.A., Thompson, W.F., Conkling, M.A., 1999. Transposon tagging of the sulfur gene of tobacco using engineered maize Ac/Ds elements. Genetics 153, 1919–1928.

Geering, A.D., Thomas, J.E., 1999. Characterisation of a virus from Australia that is closely related to papaya mosaic potexvirus. Arch. Virol. 144, 577–592.

Goodin, M.M., Dietzgen, R.G., Schichnes, D., Ruzin, S., Jackson, A.O., 2002. pGD vectors: versatile tools for the expression of green and red fluorescent protein fusions in agroinfiltrated plant leaves. Plant J. 31, 375–383.
Goulden, M.G., Kohm, B.A., Santa Cruz, S., Kavanagh, T.A., Baulcombe, D.C., 1993. A feature of the coat protein of *Potato virus X* affects both induced virus resistance in potato and viral fitness. Virology 197, 293–302.
Hajimorad, M.R., Eggenberger, A.L., Hill, J.H., 2005. Loss and gain of elicitor function of *Soybean mosaic* virus G7 provoking Rsv1-mediated lethal systemic hypersensitive response maps to P3. J Virol. 79, 1215–1222.
Hammond, J., Reinsel, M.D., Maroon-Lango, C.J., 2006a. Identification and full sequence of an isolate of *Alternanthera mosaic* potexvirus infecting *Phlox stolonifera*. Arch. Virol. 151, 477–493.
Hammond, J., Reinsel, M.D., Maroon-Lango, C.J., 2006b. Identification of potexvirus isolates from phlox and portulaca as strains of *Alternanthera mosaic virus*. Acta Hortic. 722, 71–77.
Hartl, M., Merker, H., Schmidt, D.D., Baldwin, I.T., 2008. Optimized virus-induced gene silencing in *Solanum nigrum* reveals the defensive function of leucine aminopeptidase against herbivores and the shortcomings of empty vector controls. N. Phytol. 179, 356–365.
Hashimoto, M., Komatsu, K., Maejima, K., Okano, Y., Shiraishi, T., Ishikawa, K., Takinami, Y., Yamaji, Y., Namba, S., 2012. Identification of three MAPKKKs forming a linear signaling pathway leading to programmed cell death in *Nicotiana benthamiana*. BMC Plant Biol. 12, 103.
James, P., Halladay, J., Craig, E.A., 1996. Genomic libraries and a host strain designed for highly efficient two-hybrid selection in yeast. Genetics 144, 1425–1436.
Jin, H., Axtell, M.J., Dahlbeck, D., Ekwenna, O., Zhang, S., Staskawicz, B., Baker, B., 2002. NPK1, an MEKK1-like mitogen-activated protein kinase kinase kinase, regulates innate immunity and development in plants. Dev. Cell 3, 291–297.
Jin, H., Liu, Y., Yang, K.-Y., Kim, C.Y., Baker, B., Zhang, S., 2003. Function of a mitogen-activated protein kinase pathway in N gene-mediated resistance in tobacco. Plant J. 33, 719–731.
Kagiwada, S., Yamaji, Y., Komatsu, K., Takahashi, S., Mori, T., Hirata, H., Suzuki, M., Ugaki, M., Namba, S., 2005. A single amino acid residue of RNA-dependent RNA polymerase in the *Potato virus X* genome determines the symptoms in *Nicotiana* plants. Virus Res. 110, 177–182.
Kendall, A., Bian, W., Maris, A., Azzo, C., Groom, J., Williams, D., Shi, J., Stewart, P.L., Wall, J.S., Stubbs, G., 2013. A common structure for the potexviruses. Virology 436, 173–178.
Király, L., Cole, A.B., Bourque, J.E., Schoelz, J.E., 1999. Systemic cell death is elicited by the interaction of a single gene in *Nicotiana clevelandii* and gene VI of *Cauliflower mosaic virus*. Mol. Plant–Microbe Interact. 12, 919–925.
Komatsu, K., Hashimoto, M., Ozeki, J., Yamaji, Y., Maejima, K., Senshu, H., Himeno, M., Okano, Y., Kagiwada, S., Namba, S., 2010. Viral-induced systemic necrosis in plants involves both programmed cell death and the inhibition of viral multiplication, which are regulated by independent pathways. Mol. Plant–Microbe Interact. 23, 283–293.
Komatsu, K., Hashimoto, M., Maejima, K., Shiraishi, T., Neriya, Y., Miura, C., Minato, N., Okano, Y., Sugawara, K., Yamaji, Y., Namba, S., 2011. A necrosis-inducing elicitor domain encoded by both symptomatic and asymptomatic *Plantago asiatica mosaic virus* isolates, whose expression is modulated by virus replication. Mol. Plant–Microbe Interact. 24, 408–420.
Laliberté Gagné, M.E., Lecours, K., Gagné, S., Leclerc, D., 2008. The F13 residue is critical for interaction among the coat protein subunits of papaya mosaic virus. FEBS J. 275, 1474–1484.
Lim, H.S., Bragg, J.N., Ganesan, U., Ruzin, S., Schichnes, D., Lee, M.Y., Vaira, A.M., Ryu, K.H., Hammond, J., Jackson, A.O., 2009. Subcellular localization of the barley stripe mosaic virus triple gene block proteins. J. Virol. 83, 9432–9448.
Lim, H.S., Vaira, A.M., Reinsel, M.D., Bae, H., Bailey, B.A., Domier, L.L., Hammond, J., 2010a. Pathogenicity of *Alternanthera mosaic virus* is affected by determinants in RNA-dependent RNA polymerase and by reduced efficacy of silencing suppression in a movement-competent TGB1. J. Gen. Virol. 91, 277–287.
Lim, H.S., Vaira, A.M., Domier, L.L., Lee, S.C., Kim, H.G., Hammond, J., 2010b. Efficiency of VIGS and gene expression in a novel bipartite potexvirus vector delivery system as a function of strength of TGB1 silencing suppression. Virology 402, 149–163.
Lockhart, B.E., Daughtrey, M.L., 2008. First report of *Alternanthera mosaic virus* infection in Angelonia in the United States. Plant Dis. 92, 1473.
Lukashina, E., Ksenofontov, A., Fedorova, N., Badun, G., Mukhamedzhanova, A., Karpova, O., Rodionova, N., Baratova, L., Dobrov, E., 2012. Analysis of the role of the coat protein N-terminal segment in Potato virus X virion stability and functional activity. Mol. Plant Pathol. 13, 38–45.
Moffett, P., Farnham, G., Peart, J., Baulcombe, D.C., 2002. Interaction between domains of a plant NBS-LRR protein in disease resistance-related cell death. EMBO J. 21, 4511–4519.
Mukhamedzhanova, A.A., Smirnov, A.A., Arkhipenko, M.V., Ivanov, P.A., Chirkov, S.N., Rodionova, N.P., Karpova, O.V., Atabekov, J.G., 2011. Characterization of *Alternanthera mosaic virus* and its coat protein. Open Virol. J. 5, 136–140.
Nable, R.O., Bañuelos, G.S., Paull, J.G., 1997. Boron toxicity. Plant Soil 193, 181–198.
Ozeki, J., Takahashi, S., Komatsu, K., Kagiwada, S., Yamashita, K., Mori, T., Hirata, H., Yamaji, Y., Ugaki, M., Namba, S., 2006. A single amino acid in the RNA-dependent RNA polymerase of *Plantago asiatica mosaic virus* contributes to systemic necrosis. Arch. Virol. 151, 2067–2075.
Padgett, H.S., Watanabe, Y., Beachy, R.N., 1997. Identification of the TMV replicase sequence that activates the *N* gene-mediated hypersensitive response. Mol. Plant–Microbe Interact. 10, 709–715.
Palanichelvam, K., Cole, A.B., Shababi, M., Schoelz, J.E., 2000. Agroinfiltration of *Cauliflower mosaic virus* gene VI elicits hypersensitive response in *Nicotiana* species. Mol. Plant–Microbe Interact. 13, 1275–1279.
Park, S.-H., Kim, K.-H., 2012. Virus-induced silencing of the WRKY1 transcription factor that interacts with the SL1 structure of *Potato virus X* leads to higher viral RNA accumulation and severe necrotic symptoms. Plant Pathol. J. 28, 40–48.
Peart, J.R., Lu, R., Sadanandom, A., Malcuit, I., Moffett, P., Brice, D.C., Schauser, L., Jaggard, D.A., Xiao, S., Coleman, M.J., Dow, M., Jones, J.D., Shirasu, K., Baulcombe, D.C., 2002. Ubiquitin ligase-associated protein SGT1 is required for host and nonhost disease resistance in plants. Proc. Natl. Acad. Sci. USA 99, 10865–10869.
Petty, I.T., Hunter, B.G., Wei, N., Jackson, A.O., 1989. Infectious *Barley stripe mosaic virus* RNA transcribed *in vitro* from full-length genomic cDNA clones. Virology 171, 342–349.
Querci, M., van der Vlugt, R., Goldbach, R., Salazar, L.F., 1993. RNA sequence of potato virus X strain HB. J. Gen. Virol. 74, 2251–2255.
Ratcliff, F., Martin-Hernandez, A.M., Baulcombe, D.C., 2001. Technical advance. *Tobacco rattle virus* as a vector for analysis of gene function by silencing. Plant J. 25, 237–245.
Rodriguez, M.C.S., Petersen, M., Mundy, J., 2010. Mitogen-activated protein kinase signaling in plants. Annu. Rev. Plant Biol. 61, 621–649.
Scholthof, H.B., Scholthof, K.B., Jackson, A.O., 1995. Identification of *Tomato bushy stunt virus* host-specific symptom determinants by expression of individual genes from a *Potato virus X* vector. Plant Cell 7, 1157–1172.
Seo, J.K., Lee, S.H., Kim, K.H., 2009. Strain-specific cylindrical inclusion protein of *Soybean mosaic virus* elicits extreme resistance and a lethal systemic hypersensitive response in two resistant soybean cultivars. Mol. Plant–Microbe Interact. 22, 1151–1159.
Someya, N., Niinuma, K., Kimura, M., Yamaguchi, I., Hamamoto, H., 2004. Pattern of N gene-mediated systemic hypersensitive response and turnover of viral replicase protein in tobacco. Arch. Virol. 149, 2105–2113.
Sturbois, B., Dubrana-Ourabah, M.P., Gombert, J., Lasseur, B., Macquet, A., Faure, C., Bendahmane, A., Baurès, I., Candresse, T., 2012. Identification and characterization of tomato mutants affected in the Rx-mediated resistance to PVX isolates. Mol. Plant–Microbe Interact. 25, 341–354.
Takano, J., Noguchi, K., Yasumori, M., Kobayashi, M., Gajdos, Z., Miwa, K., Hayashi, H., Yoneyama, T., Fujiwara, T., 2002. Arabidopsis boron transporter for xylem loading. Nature 420, 337–340.
Takano, J., Miwa, K., Yuan, L., von Wirén, N., Fujiwara, T., 2005. Endocytosis and degradation of BOR1, a boron transporter of *Arabidopsis thaliana*, regulated by boron availability. Proc. Natl. Acad. Sci. USA 102, 12276–12281.
Tameling, W.I., Baulcombe, D.C., 2007. Physical association of the NB-LRR resistance protein Rx with a Ran GTPase-activating protein is required for extreme resistance to *Potato virus X*. Plant Cell 19, 1682–1694.
Tameling, W.I., Nooijen, C., Ludwig, N., Boter, M., Slootweg, E., Goverse, A., Shirasu, K., Joosten, M.H., 2010. RanGAP2 mediates nucleocytoplasmic partitioning of the NB-LRR immune receptor Rx in the *Solanaceae*, thereby dictating Rx function. Plant Cell 22, 4176–4194.
Taraporewala, Z.F., Culver, J.N., 1996. Identification of an elicitor active site within the three-dimensional structure of the tobacco mosaic tobamovirus coat protein. Plant Cell 8, 169–178.
Toedt, J.M., Braswell, E.H., Schuster, T.M., Yphantis, D.A., Taraporewala, Z.F., Culver, J.N., 1999. Biophysical characterization of a designed TMV coat protein mutant, R46G, that elicits a moderate hypersensitivity response in *Nicotiana sylvestris*. Protein Sci. 8, 261–270.
Tremblay, M.H., Majeau, N., Gagné, M.E., Lecours, K., Morin, H., Duvignaud, J.B., Bolduc, M., Chouinard, N., Paré, C., Gagné, S., Leclerc, D., 2006. Effect of mutations K97A and E128A on RNA binding and self assembly of papaya mosaic potexvirus coat protein. FEBS J. 273, 14–25.
Waadt, R., Schmidt, L.K., Lohse, M., Hashimoto, K., Bock, R., Kudla, J., 2008. Multicolor bimolecular fluorescence complementation reveals simultaneous formation of alternative CBL/CIPK complexes in planta. Plant J. 56, 505–516.
Wimmer, M.A., Lochnit, G., Bassil, E., Mühling, K.H., Goldbach, H.E., 2009. Membrane-associated, boron-interacting proteins isolated by boronate affinity chromatography. Plant Cell Physiol. 50, 1292–1304.
Wurch, T., Lestienne, F., Pauwels, P., 1998. A modified overlap extension PCR method to create chimeric genes in the absence of restriction enzymes. Biotechnol. Tech. 12, 653–657.
Yang, S., Wang, T., Bohon, J., Gagné, M.È., Bolduc, M., Leclerc, D., Li, H., 2012. Crystal structure of the coat protein of the flexible filamentous papaya mosaic virus. J. Mol. Biol. 422, 263–273.